© 2014. Published by The Company of Biologists Ltd | Development (2014) 141, 1950-1960 doi:10.1242/dev.104166

RESEARCH ARTICLE

# Cadherin 99C regulates apical expansion and cell rearrangement during epithelial tube elongation

**SeYeon Chung and Deborah J. Andrew***


## ABSTRACT

Apical and basolateral determinants specify and maintain membrane domains in epithelia. Here, we identify new roles for two apical surface proteins – Cadherin 99C (Cad99C) and Stranded at Second (SAS) – in conferring apical character in *Drosophila* tubular epithelia. Cad99C, the *Drosophila* ortholog of human Usher protocadherin PCDH15, is expressed in several embryonic tubular epithelial structures. Through loss-of-function and overexpression studies, we show that Cad99C is required to regulate cell rearrangement during salivary tube elongation. We further show that overexpression of either Cad99C or SAS causes a dramatic increase in apical membrane at the expense of other membrane domains, and that both proteins can do this independently of each other and independently of mislocalization of the apical determinant Crumbs (Crb). Overexpression of Cad99C or SAS results in similar, but distinct effects, suggesting both shared and unique roles for these proteins in conferring apical identity.


**KEY WORDS: Apicobasal polarity, Epithelial organ development, Salivary gland, Tubulogenesis, *Drosophila***

## INTRODUCTION

Epithelial tissues in multicellular organisms are manifested by apicobasal polarity, which is essential for their correct form and function (Laprise and Tepass, 2011; St. Johnston and Ahringer, 2010; Tepass, 2012). In polarized epithelia, the apical domain faces the outside world or the tube lumen, and is separated by junctional structures from other membrane domains. The basal and lateral domains, often referred to collectively as the 'basolateral' domain, are distinct, with the lateral domain contacting neighboring cells through adhesion molecules and the basal domain contacting an underlying extracellular matrix (ECM) or cells of other tissues.

*Drosophila* epithelia have been instrumental in identifying polarity regulators and revealing the mechanisms underlying the establishment and maintenance of polarity. The known polarity regulators localize in complexes located in specific regions along the lateral cell surface. Apical determinants, including the Crumbs (Crb/Sdt/Patj/Lin7) and atypical Protein kinase C (aPKC/Par3/Par6) complexes, are enriched in the sub-apical region (SAR), the small region of cell-cell contact apical to the adherens junctions (AJs) (Tepass, 1996, 2012; Wodarz et al., 2000). The Scribble complex (Scrib/Lgl/Dlg), which specifies basolateral identity, localizes to the septate junction (SJ) region, immediately basal to the AJs, along with known SJ components (Bilder and Perrimon, 2000; Strand et al., 1994; Woods and Bryant, 1991). Mutually competitive, negative feedback between these apical and basolateral regulators limits each polarity domain (Tepass, 2012). Interestingly, only very few apical surface proteins have been identified (Baumgartner et al., 1996; Jaźwińska et al., 2003; Zhang and Ward, 2009) and their importance in cell polarity and organ shape has not been addressed.

*Drosophila* tubular epithelia include tissues that differentiate into organs with specific functions, such as secretion (e.g. the salivary gland, SG) or gas exchange (e.g. the trachea) (Maruyama and Andrew, 2012). These tubular organs form directly from already polarized ectodermal epithelia, which exhibit discrete subcellular localization of polarity complexes and other junctional proteins. The SGs form from two primordia of ~150 surface ectodermal cells found in the ventral region of parasegment two, the most posterior region of the head. Over a period of a few hours, the SG primordia invaginate, elongate and collectively migrate to form simple unbranched tubes (Maruyama and Andrew, 2012). The large cell size and simple structure, as well as the absence of cell division and cell death, make the *Drosophila* SG ideal for examining how changes in cell shape, adhesion and position affect tube morphology.

Cadherin 99C (Cad99C), the *Drosophila* ortholog of the human Usher syndrome-linked protein protocadherin 15, localizes to the apical surface of several simple undifferentiated epithelia, including ovarian follicle and wing imaginal disc cells (D'Alterio et al., 2005; Schlichting et al., 2005; Schlichting et al., 2006). Cad99C regulates microvillar length in follicle cells, with *Cad99C* loss reducing microvillar length and overexpression increasing microvillar length (D'Alterio et al., 2005; Schlichting et al., 2006). We understand very little about how Cad99C controls membrane dynamics and we do not know if or how this protein functions in other epithelial tissues. Similarly, the role of the Stranded at Second (SAS) protein, which also localizes to the apical surface of many epithelial tissues (Schonbaum et al., 1992), is unknown. Here, we explore the roles of both proteins in tubular epithelia. We show through loss and overexpression studies that Cad99C affects cell rearrangement during tube elongation in the *Drosophila* SG and that overexpression of either Cad99C or SAS confers apical identity on other membrane domains.

## RESULTS

### Cad99C loss affects cell rearrangement

Staining of *Drosophila* embryonic SGs with known polarity components revealed that SAS localizes most apically, occupying the apical surface, which directly contacts the lumen (Fig. 1A). Along the lateral surface, the most apical staining was observed in the SAR with Crb (Fig. 1B) and other components of the Crb complex (data not shown). E-Cadherin (E-Cad) staining – along with other AJ components – was observed immediately basal to the SAR (Fig. 1B; data not shown). SJ markers, such as Coracle (Cora) (Lamb et al., 1998), and the basolateral determinants Scrib, Dlg and Lgl (Bilder and Perrimon, 2000; Strand et al., 1994; Woods and Bryant, 1991) localized just basal to the AJ (Fig. 1C,D; data not

Department of Cell Biology, The Johns Hopkins University School of Medicine, 725 North Wolfe Street, Baltimore, MD 21205-2196, USA.

*Author for correspondence (dandrew@jhmi.edu)

**Received 24 September 2013; Accepted 10 March 2014**

Development (2014) 141, 1950-1960 doi:10.1242/dev.104166

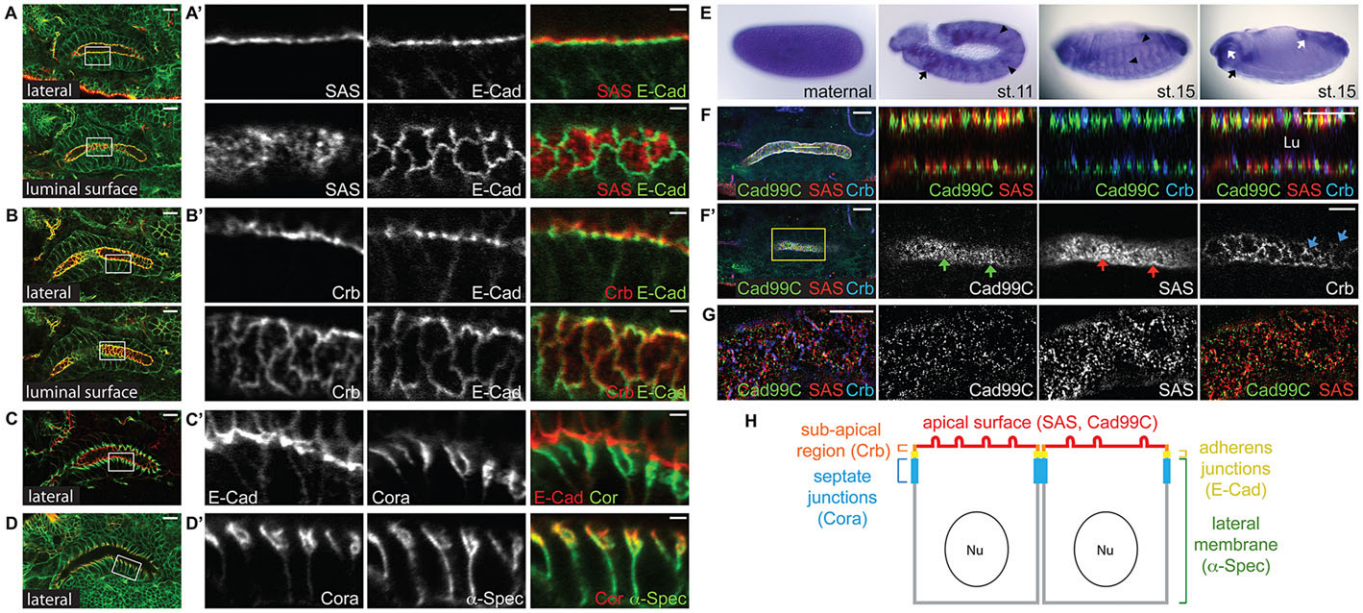


**Fig. 1. *Cad99C* is expressed in embryos and the protein localizes to the SG apical surface membrane.** (A-D′) Confocal images of stage 16 wild-type SGs stained with different polarity and junctional markers. (A,A′) SAS (red) and E-Cad (green). (B,B′) Crb (red) and E-Cad (green). (C,C′) E-Cad (red) and Cora (green). (D,D′) Cora (red) and α-Spec (green). (E) *Cad99C* mRNA is maternally contributed (left panel). From stage 11, *Cad99C* is expressed in several tubular organs, including the SG (black arrows), trachea (arrowheads), and foregut and hindgut derivatives (white arrows). Images in the last two panels are the same embryo at different focal planes. (F,F′) Confocal images of stage 16 SGs stained with Cad99C (green), Crb (cyan) and SAS (red). (F) A confocal projection image. Right panels show higher magnifications of an orthogonal section. Cad99C and SAS localize along the entire apical surface, but only occasionally overlap. Lu, lumen. (F′) A luminal surface view of the same gland in F. Crb is enriched at the SAR (cyan arrows), whereas Cad99C (green arrows) and SAS (red arrows) are localized along the entire apical surface. (G) Super-resolution images of Cad99C, SAS and Crb in a wild-type SG confirmed mostly non-overlapping Cad99C and SAS localization. (H) SG epithelial cells showing distinct membrane domains and domain-specific proteins. Scale bars: 10 μm in A-D, left panels of F and F′; 5 μm in A′-D′, G, right panels in F,F′.

shown). Finally, the lateral membrane-associated protein α-Spectrin (α-Spec) localized along the entire lateral domain (Fig. 1D).

*Cad99C* mRNA is maternally contributed and, at later embryonic stages, is expressed in several tubular organs, including the SG, trachea, foregut and hindgut (Fig. 1E). As observed with SAS, Cad99C protein localized to the apical surface in the SG and other tubular organs, distinct from the sub-apical localization of Crb (Fig. 1F) and consistent with its localization in follicle cells and imaginal discs (D'Alterio et al., 2005; Schlichting et al., 2005; Schlichting et al., 2006). Super-resolution images revealed that Cad99C and SAS are mostly non-overlapping, indicating that the two proteins occupy distinct regions on the apical surface (Fig. 1G).

Cad99C expression in developing tubular organs led us to examine Cad99C function in the SG. Most embryos from homozygous mutant females ($Cad99C^{M}$) are not recoverable, whether the females are crossed to *Cad99C* mutant or to wild-type males, as Cad99C is required for eggshell integrity (D'Alterio et al., 2005; Schlichting et al., 2006). Surprisingly, most (>90%) of the $Cad99C^{M/Z}$ embryos we did recover (from crosses of homozygous females and males) developed relatively normally but had longer, thinner SG lumens than wild type (Fig. 2A,B); only a small subset of the recovered $Cad99C^{M/Z}$ embryos showed severe morphological defects (supplementary material Fig. S1). Embryos missing only maternal (*Cad99C* mutant females crossed to wild-type males) or only zygotic function (heterozygous *Cad99C* mutants crossed to each other) did not have overt defects, suggesting that either maternal or zygotic function of Cad99C is sufficient for embryonic development (data not shown).

To investigate the cellular basis for the longer thinner SGs observed in $Cad99C^{M/Z}$ embryos, we carried out transmission electron microscopy (TEM) analysis using the high-pressure freezing (HPF) method that allows better preservation of cellular membranes than traditional fixation methods (McDonald and Auer, 2006). We also carried out confocal imaging with a variety of polarity and tissue-specific markers. No phenotypic differences were detected at the ultrastructural level in comparisons of stage 15/16 $Cad99C^{M/Z}$ mutant and wild-type SGs (Fig. 2C). Moreover, overall polarity of $Cad99C^{M/Z}$ mutant SGs appeared unaffected and the mutant SGs migrated normally, contacting the same tissues at all stages as wild-type SGs (Fig. 2E; data not shown). Total cell numbers were not significantly different (Table 1), and the apical domain size and elongation ratio of individual cells were also unchanged (Fig. 2D,F). Indeed, the only difference was that fewer cells surrounded the lumen in cross-sections of the $Cad99C^{M/Z}$ mutant SGs compared with wild type (Fig. 2E; Table 1). Thus, the longer, thinner SG lumens in $Cad99C^{M/Z}$ mutants reflect differences in cell rearrangement during tube elongation.

### Cad99C overexpression affects cell rearrangement and expands the apical surface membrane

Overexpression of full-length Cad99C protein (Cad99C-FL; D'Alterio et al., 2005) in otherwise wild-type SGs using *fork head* (*fkh*)-Gal4 (Henderson and Andrew, 2000) resulted in a dramatic expansion of luminal width with differences first visible during invagination (Fig. 3A,B) and more obvious in late embryos (Fig. 3C-F). The apical domain of individual cells in Cad99C-FL-overexpressing SGs was expanded significantly (Fig. 3F), with the apical membranes extending deep into the lateral regions on the apical side, where staining of all tested apical markers was observed, including SAS, Crb, aPKC and $\beta_H$-spectrin (Fig. 3D,E; data not shown). TEM analysis of stage 15/16 Cad99C-FL-overexpressing

Development (2014) 141, 1950-1960 doi:10.1242/dev.104166

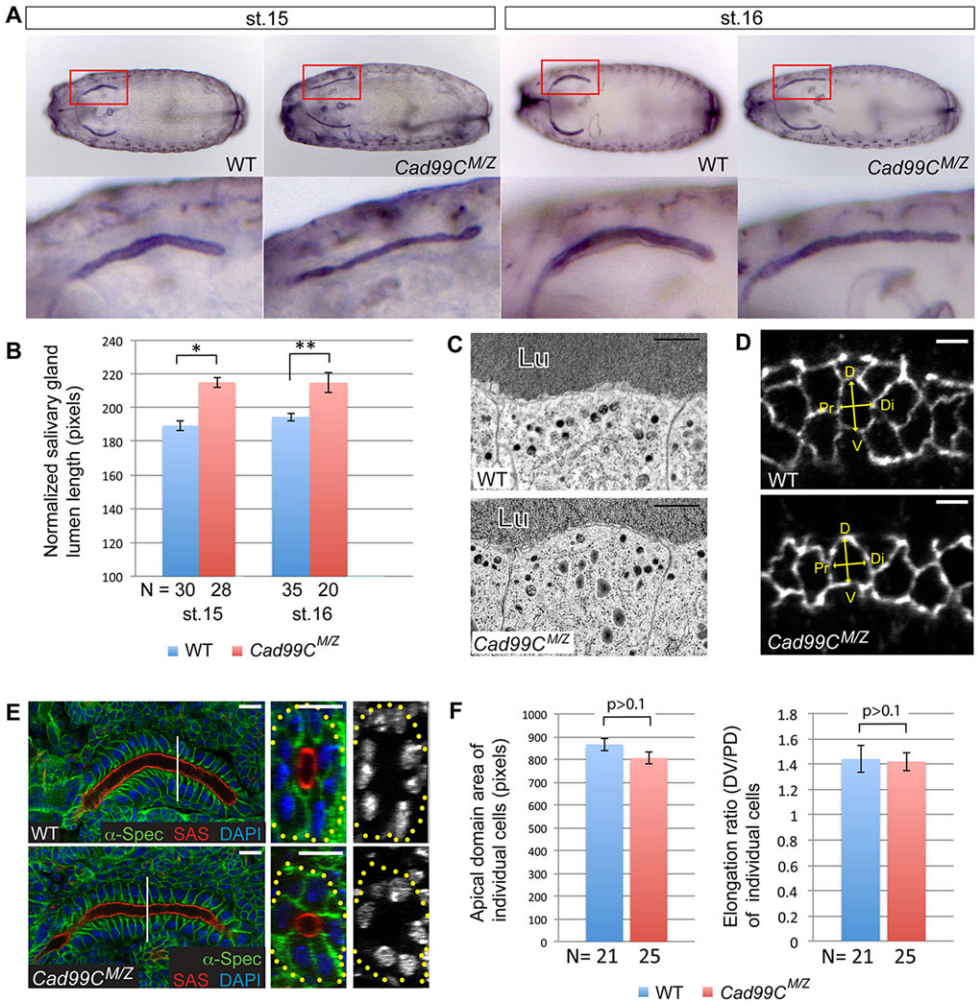


**Fig. 2. *Cad99C*$^{M/Z}$ mutants have longer thinner SG lumens.** (A) *Cad99C*$^{M/Z}$ embryos have over-elongated SGs (stained with Crb). (B) Quantification of the SG luminal length in wild type and *Cad99C*$^{M/Z}$ mutants normalized to overall embryo length. N, number of SGs measured. Error bars indicate s.e.m. *$P<10^{-6}$; **$P<0.0005$. (C) TEM images of apical region of the stage 15 SG cells. Lu, lumen. (D) Confocal images of E-Cad staining in stage 16 wild-type and *Cad99C*$^{M/Z}$ SGs were acquired to measure the apical domain size and the elongation ratio of individual cells. D, dorsal; V, ventral; Pr, proximal; Di, distal. (E) Single sections of confocal images of wild-type and *Cad99C*$^{M/Z}$ mutant SGs stained with SAS (red), α-Spec (green) and DAPI (blue). Cross-sections at the levels of the white bars are shown in the right panels. (F) Apical domain size and the elongation ratio. N, number of cells measured from five or more different SGs. Error bars indicate s.e.m. Scale bars: 1 μm in C; 2 μm in D; 10 μm in E.

SGs revealed increases in apical, microvilli-like structures extending into the lumen, as well as in apical membrane protruding deep into the regions between cells (Fig. 3G). Interestingly, the apical ECM appeared less regular in Cad99C-overexpressing SGs, with large regions of very sparse electron-dense material (Fig. 3G). Importantly, confocal cross-sections of Cad99C-FL-overexpressing SGs revealed many more cells surrounding the lumen than in wild type (Fig. 3H; Table 1), indicating that cell rearrangement during tube elongation is also affected by Cad99C overexpression. Overall luminal length of Cad99C-FL-overexpressing SGs was not significantly different from wild type despite the apical expansion of individual cells, likely reflecting some length compensation due to the defects in cell arrangement observed in Cad99C-FL overexpressing SGs relative to wild type (Fig. 3F).

**Table 1. Quantification of the nuclei in the SGs**

| Genotype | Total numbers of nuclei in the SG | Numbers of nuclei around the lumen in cross-sections |
|---|---|---|
| Wild type | 144±1.4 (10) | 7.8±0.1 (7) |
| *Cad99C*$^{M/Z}$ | 145.4±4.1 (8) | 6.7±0.3 (5)* |
| *fkh>Cad99C-FL* | 145.1±2.2 (10) | 10.6±0.4 (6)** |
| *fkh>Cad99CΔCyt* | 146.2±1.5 (10) | 7.9±0.2 (6) |

Data are mean±s.e.m.
Numbers of the SGs counted are shown in parenthesis.
*$P<0.005$; **$P<10^{-4}$; $P>0.1$ for others.

Intriguingly, morphological changes associated with Cad99C-FL overexpression were not confined to the apical domain. Throughout embryogenesis, Cad99C-overexpressing SGs had irregular basal boundaries, with indentations between individual cells, distinct from the smooth basal surfaces of controls (Fig. 3B). By late embryogenesis, several Cad99C-overexpressing cells had lost the typical columnar shape and were either cuboidal or round, with minimal contact between neighbors (Fig. 3D). The rounded cells always had mislocalized Cad99C signals in the basal domain. Overexpression of either Cad99C-FL or Cad99C-FL-GFP (Schlichting et al., 2006) in the trachea using *breathless* (*btl*)-Gal4 (Shiga et al., 1996) resulted in similar phenotypes, including apical membrane expansion and cell rounding that correlated with mislocalized Cad99C in the basal membrane, suggesting a conserved role for Cad99C in different tubular epithelia (supplementary material Fig. S2).

### The extracellular domain of Cad99C confers apical character

Rounded basal domains were invariably associated with Cad99C mislocalization to the basal membrane, and with weak/punctate overlapping SAS staining (Fig. 4B-E). These phenotypes are reminiscent of the overexpression phenotype of Crb, a known apical determinant, in epidermal cells (Wodarz et al., 1995). Crb overexpression in SGs also expanded the lumen and caused the basal domain to acquire apical character, based on SAS mislocalization

Development (2014) 141, 1950-1960 doi:10.1242/dev.104166

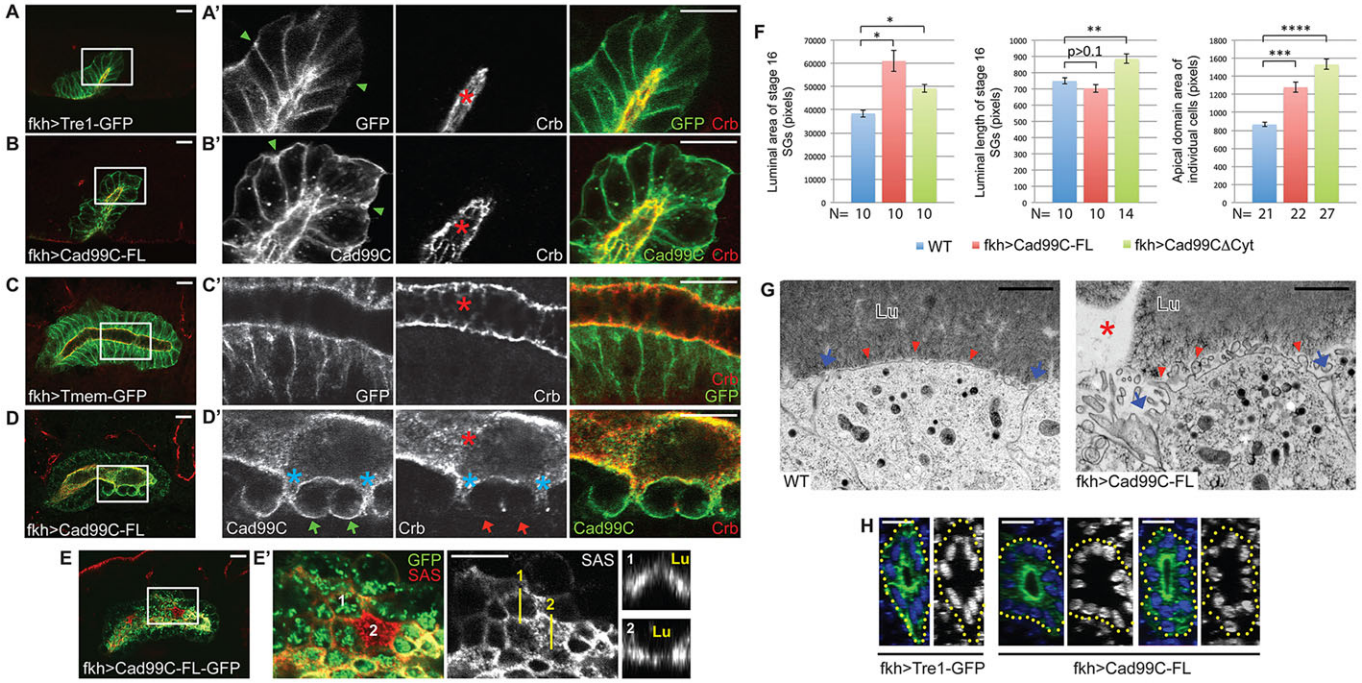


**Fig. 3. Cad99C overexpression expands apical membranes and affects cell rearrangements.** (A-D′) Single confocal sections of SGs expressing Tre1-GFP or Tmem-GFP (A,A′,C,C′) or Cad99C (B,B′,D,D′) under the control of *fkh*-Gal4, which drives SG expression shortly after SGs are specified (Henderson and Andrew, 2000). Crb marks apical membranes (red asterisks). (A-B′) Stage 11 SGs. Green arrowheads indicate the smooth (control) or irregular/rounder (Cad99C-overexpressing) basal surfaces. (C-D′) Stage 16 SGs. Apical membranes protrude into the lateral domain (cyan asterisks). Cad99C is mislocalized to the basal domain of the rounded cells (green arrows), but Crb is barely detectable (red arrows). (E,E′) Confocal images of a GFP-tagged Cad99C-overexpressing stage 16 SG. SAS (red) marks the apical membrane. Compare the convex apical surface of the Cad99C-overexpressing cell (cell 1) with the flat apical surface of the neighboring wild-type non-expressing cell (cell 2; note the absence of GFP signals). (F) The luminal area (N, the number of SGs), luminal length (N, the number of SGs) and the apical domain size of individual cells (N, the number of cells measured from three to six different SGs). Error bars indicate s.e.m. *$P$<0.0005; **$P$<0.005; ***$P$<$10^{-7}$; ****$P$<$10^{-12}$. (G) TEM images of the apical region of stage 16 wild-type and Cad99C-FL-expressing SGs. Lu, lumen. Compared with wild type, the apical ECMs in Cad99C-FL-overexpressing SGs are less regular, with large regions of very sparse electron-dense material (red asterisks). Cad99C-FL-overexpressing SG cells have many more microvillar-like extensions of the apical membrane (red arrowheads) and the apical domain is rounder, protruding into the lateral domain (blue arrows). (H) Cross-sections of confocal images of Tre1-GFP- (control) and Cad99C-FL-overexpressing SGs reveal the number of nuclei/cells around a cross-section of the lumen. Yellow dots mark the boundary of the gland. Scale bars: 10 μm in A-E′,H; 2 μm in G.

(Fig. 4F). Interestingly, Cad99C was not detected in the ‘converted’ domain where Crb and SAS mislocalized (Fig. 4F). Similarly, Crb was barely detectable in the ‘converted’ apical domain observed with Cad99C overexpression (Fig. 3D), suggesting that the mislocalized SAS observed with Cad99C overexpression is not caused by Crb mislocalization.

To investigate the function of the extra- and intracellular domains of Cad99C, we expressed each using *fkh*-Gal4 (Fig. 4A; supplementary material Fig. S3A). Cad99CΔCyt (Schlichting et al., 2006) overexpression resulted in apical SG membrane expansion (Figs 3F and 4G), but overexpressed Cad99CΔEx (Schlichting et al., 2006) did not affect SG morphology (supplementary material Fig. S3C). Confocal and TEM analyses revealed that Cad99CΔCyt expression in SGs, like Cad99C-FL, increases microvilli-like structures and causes apical membranes to protrude into the lateral domain (Fig. 4G,H).

Some phenotypes of Cad99CΔCyt overexpression were distinct from those resulting from Cad99C-FL overexpression. The tubes were longer than with Cad99C-FL overexpression (Fig. 3F) and the average number of nuclei per cross-section was not significantly different in Cad99CΔCyt-overexpressing compared with wild-type SGs, suggesting normal cell rearrangement (Fig. 4I; Table 1). Strikingly, in Cad99CΔCyt-expressing SGs, Cad99C signals were highest in the basal region (Fig. 4G). As the Cad99CΔEx protein localized apically (supplementary material Fig. S3), we conclude that the cytoplasmic domain mediates apical targeting and/or retention. Cad99CΔCyt-localizing basal domains were always associated with rounded cell morphology and weak SAS mislocalization (Fig. 4G). As endogenous Cad99C protein was not observed in the basal domain when stained with a cytoplasmic region-specific antibody, and as Cad99CΔCyt overexpression in a *Cad99C*-null background resulted in the same phenotype as in a wild-type background, the observed phenotypes are not due to redistribution of the endogenous protein (data not shown). Altogether, these data suggest that the extracellular (and transmembrane) domain of Cad99C is sufficient to confer apical character on membranes but does not affect cell rearrangement during tube elongation.

### Apically targeted Cad99C colocalizes with Rab6

We expressed truncated versions of Cad99C that lack different parts of the cytoplasmic domain. Cad99CΔPBD, which lacks only the putative PDZ-binding domains, correctly localized to the apical membrane, suggesting that this domain is not required for localization (data not shown). Interestingly, Cad99CΔCyt-31, which deletes most of the cytoplasmic region leaving the 31 residues immediately after the transmembrane domain intact (D’Alterio et al., 2005), also correctly localized to the apical

Development (2014) 141, 1950-1960 doi:10.1242/dev.104166

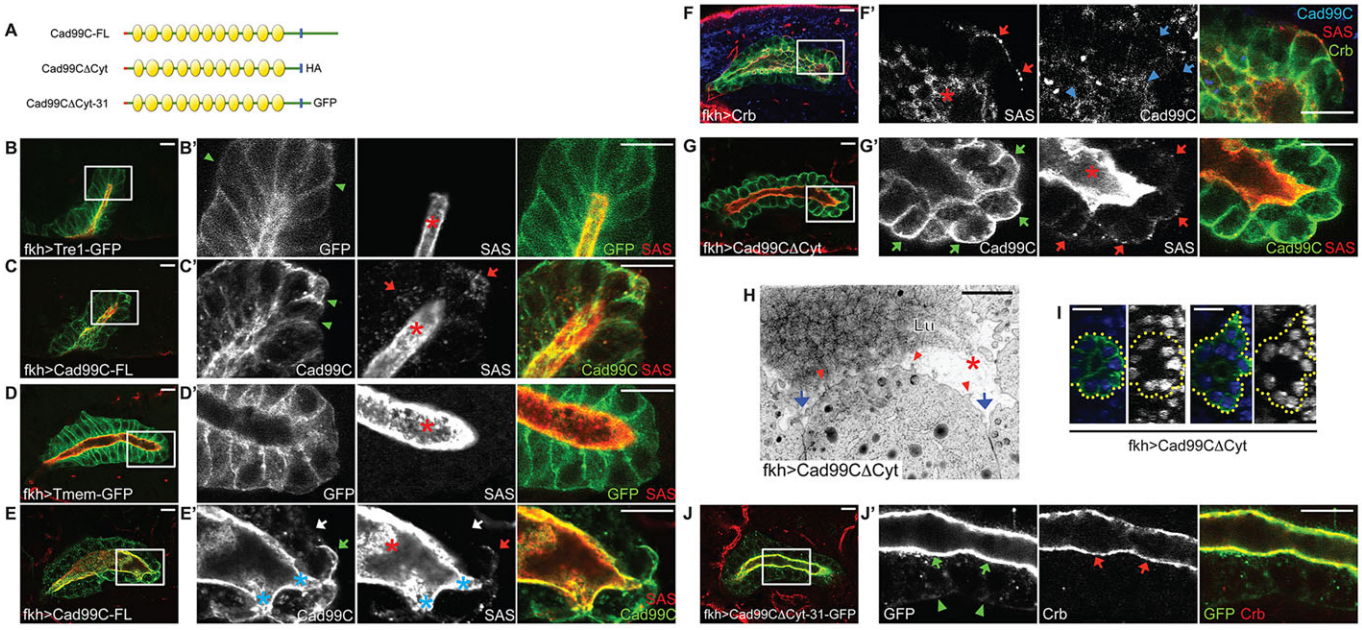


**Fig. 4. The extracellular domain of Cad99C increases apical membrane and confers apical character to other membrane domains.** (A) Full-length and truncated Cad99C proteins. The Cad99CΔCyt and Cad99CΔCyt-31 constructs have an HA or a GFP tag at the C terminus, respectively. Red bar, signal peptide; yellow ovals, cadherin repeats; blue rectangle, transmembrane domain. (B-G′,J,J′) Single sections of confocal images of SGs. (B-E′) Stage 11 (B-C′) and stage 16 (D-E′) SGs expressing Tre1-GFP or Tmem-GFP (control) or Cad99C-FL. SAS marks apical membranes (red asterisks in A-G′). Cad99C-overexpressing SGs have irregular/rounder basal surfaces compared with control (green arrowheads). Green and red arrows in C′ and E′ indicate mislocalized Cad99C and ectopic SAS signals observed in the Cad99C-expressing SG cells, respectively. SG cells that do not mislocalize Cad99C do not have ectopic SAS in the basal membrane (white arrows in E′). Cyan asterisks in E′ indicate where the apical membrane extends deep into the lateral domain. (F,F′) Stage 16 SGs overexpressing Crb stained with Crb (green), SAS (red) and Cad99C (cyan). Whereas SAS is mislocalized to the basal domain with overexpressed Crb (red arrows), dispersed Cad99C signals are detected only in the original apical domain (cyan arrowheads) and not in the basal domain (cyan arrows). (G,G′) Cad99CΔCyt signals are predominantly in the basal domain of the cells (green arrows), which are rounded and have ectopic SAS signals (red arrows). (H) TEM images of the apical region of stage 16 Cad99CΔCyt-expressing SGs. Lu, lumen. The apical ECMs in Cad99CΔCyt-overexpressing SGs are less regular (red asterisks). The apical domain of Cad99CΔCyt-overexpressing SG cells is rounder, protruding into the lateral domain (blue arrows), and has small microvillar-like structures (red arrowheads). (I) Cross-sections of confocal images of Cad99CΔCyt-overexpressing SGs reveal the number of nuclei/cells around a cross-section of the lumen. Yellow dots mark the boundary of the gland. (J,J′) Cad99CΔCyt-31 (green) localizes to the apical domain marked with Crb (red). Scale bars: 2 μm in H; 10 μm in others.

membrane, suggesting that this small juxtamembrane cytoplasmic region is sufficient for apical accumulation (Fig. 4A,J).

Cad99C overexpression causes a huge increase in vesicular structures both in the apical domain and throughout the cytoplasm, suggesting increased apical targeting (supplementary material Fig. S4B). Indeed, Cad99C overexpression resulted in dramatic increases in staining in the apical region of Rab11 and Rab6 (supplementary material Fig. S4C-F), two Rab GTPases implicated in apical trafficking (Coutelis and Ephrussi, 2007; Del Nery et al., 2006; Kerman et al., 2008; Januschke et al., 2007; Mallard et al., 2002; Martinez et al., 1997, 1994; Opdam et al., 2000; Pelissier et al., 2003; Saraste and Goud, 2007; Satoh et al., 2005; Strickland and Burgess, 2004). Consistent with the increased Rab11 and Rab6 staining, TEM analysis revealed an approximate fourfold increase in vesicles per cell slice in the apical region of Cad99C-overexpressing SG cells compared with wild type (supplementary material Fig. S4G-I). Triple labeling of Cad99C-overexpressing SG cells revealed that both Cad99C and Cad99CΔCyt vesicular staining largely overlap with Rab6 (supplementary material Fig. S4J-M).

## Newly acquired apical character affects cell and ECM architecture

To elucidate the mechanisms of the cell shape changes associated with Cad99C overexpression, we examined the distribution of junctional proteins, the actin cytoskeleton and the basal ECM. Staining with the AJ markers E-Cad and Armadillo (Arm), the *Drosophila* β-Catenin (Peifer et al., 1993), revealed that Cad99C-FL- and Cad99CΔCyt-expressing SGs have stretched AJs and wider apical domains in each cell compared with wild type (Fig. 5A-C; data not shown), consistent with increases in apical domain size (Fig. 3F). AJ markers were also detected in the expanded apical region that protrudes into the lateral domain between neighboring cells (Fig. 5B,C). Interestingly, Cad99C-FL overexpression resulted in reduced E-Cad/Arm at the apical boundaries and their dispersion throughout the apical region near the Cad99C signals (Fig. 5B; data not shown). This finding suggests that Cad99C-FL overexpression increases apical membranes at the expense of the AJ domain. Cad99CΔCyt overexpression resulted in milder affects on E-cad/Arm localization, either due to its reduced localization to the apical domain or to the absence of the cytoplasmic region. Unlike Cad99C overexpression, Crb-overexpressing SGs had punctate/spotlike AJ marker staining (Fig. 6B), further supporting the idea that Cad99C and Crb expand apical membranes by distinct mechanisms.

Cora and Dlg SJ staining patterns were narrower and extended further along the lateral membrane in both Cad99C-FL- and Cad99CΔCyt-overexpressing SGs, with more notable changes associated with Cad99CΔCyt overexpression (Fig. 5D,E). Similar patterns with SJ markers were observed in Crb-overexpressing SGs (Fig. 6A,B). Interestingly, the Cad99C- or Crb-mislocalized domains and the Cora/Dlg-localized domains were entirely non-overlapping (Fig. 5E; Fig. 6A), suggesting mutual exclusion of the 'apicalized' domain and the remaining 'lateral' domain (hereafter referred to as SJ

Development (2014) 141, 1950-1960 doi:10.1242/dev.104166

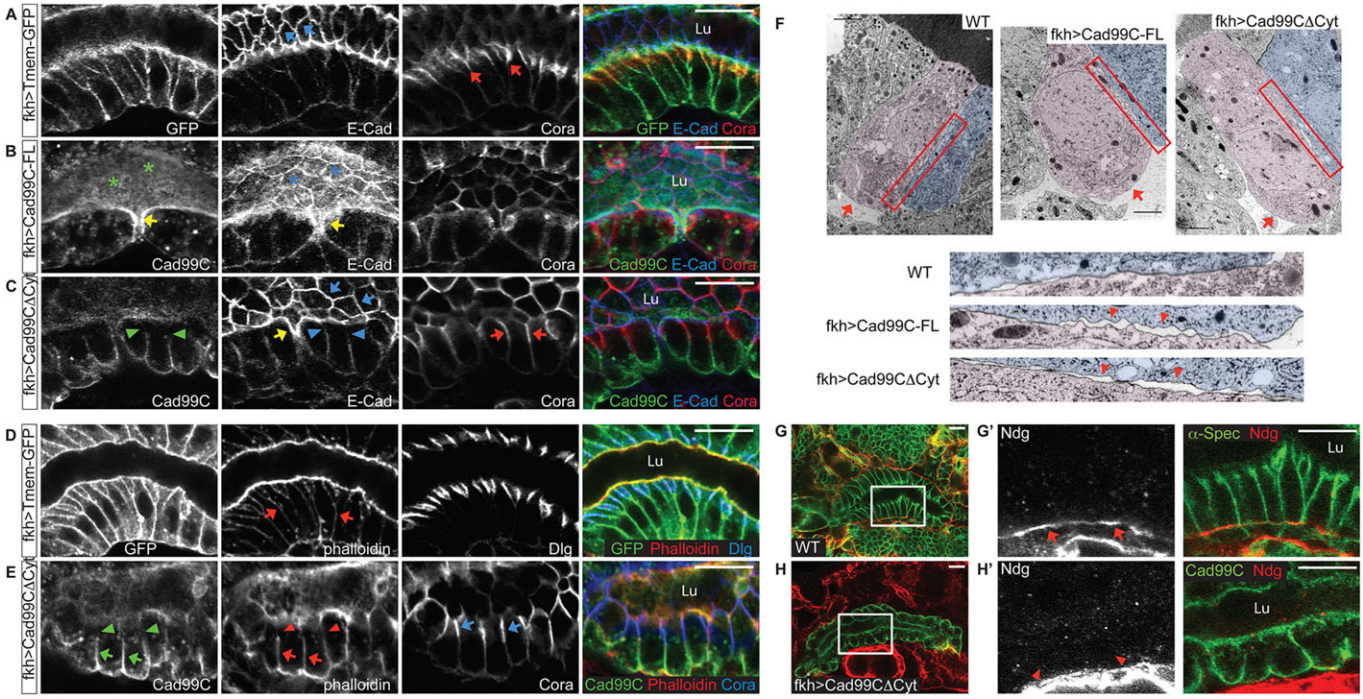


**Fig. 5. Cad99C mislocalization disrupts cell architecture and ECM deposition/accumulation on the basal surface.** (A-E,G,H) Single sections of confocal images of stage 16 SGs. (A-C) SGs stained with GFP or Cad99C (green), E-Cad (cyan) and Cora (red). E-Cad is dispersed along the apical surface membrane with Cad99C-FL overexpression (asterisks in B), but not with Cad99CΔCyt overexpression (cyan arrows in C). E-Cad is also visible at the expanded apical region between two cells (yellow arrows in B,C). With Cad99CΔCyt overexpression, SJ markers appear stretched (red arrows in C), and do not overlap with Cad99C or E-Cad (green and cyan arrowheads in C). (D,E) Compared with the uniform low-level lateral F-actin signals in wild type (red arrows in D), the lateral F-actin signals are stronger in the Cad99C-mislocalizing domains (green and red arrows in E) and weaker in the elongated SJ regions (red arrowheads and cyan arrows in E). Green arrowheads indicate the absence of Cad99C and phalloidin staining in the region of the SJs. (F) TEM images of stage 16 SG cells showing the basolateral domains. Two neighboring cells are pseudo-colored. Compared with wild type, Cad99C-FL- or Cad99CΔCyt-overexpressing cells have rounder basal domain (arrows). Higher magnifications show wider gaps between neighboring cells in Cad99C-FL- and Cad99CΔCyt-overexpressing SGs (arrowheads). (G-H′) The Ndg-stained basal ECM surrounding wild-type SGs (red arrows in G′) is not observed in the Cad99C-mislocalized SGs (red arrowheads in H′). Scale bars: 2 μm in F; 10 μm in others.

domain). Consistent with this idea, the SJ domain excluded the PH-domain of PLCδ (von Stein et al., 2005), a PtdIns(4,5)$P_2$ sensor enriched in the apical domains of fly tubular organs (Rousso et al., 2013; data not shown). SJ domains also excluded other proteins, including lateral E-Cad and F-actin; weak E-Cad and phalloidin signals were observed uniformly along the entire lateral domain in wild-type cells but were nearly absent in the SJ domains of Cad99C-overexpressing cells and were higher in the 'converted' apical domain (Fig. 5C,E). The more rounded Cad99C-overexpressing cells appeared to contact neighboring cells only through the SJ domain

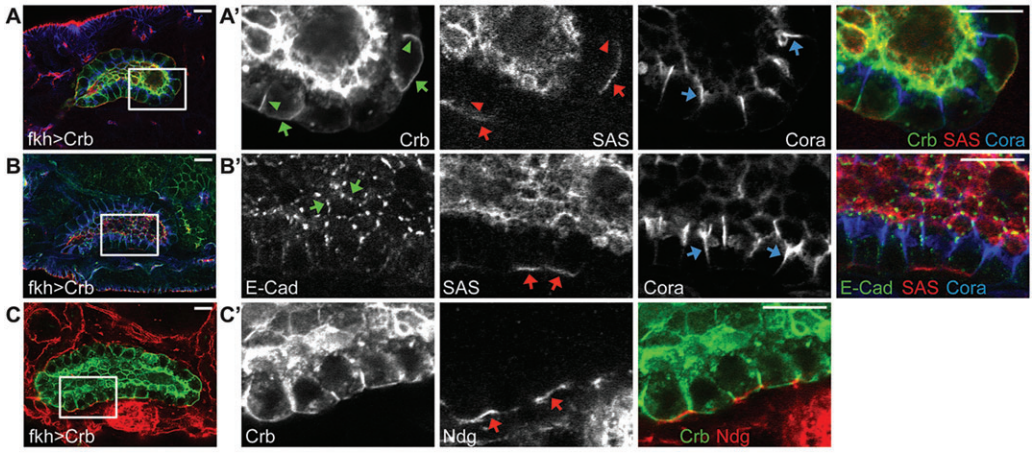


**Fig. 6. Crb overexpressing SGs have distinct phenotypes.** (A-C) Single sections of confocal images of stage 16 SGs. A′-C′ are higher magnifications of the boxed regions of A-C. (A,A′) Overexpression of Crb causes mislocalization of SAS only in the basal domain (green and red arrows), but not in the lateral domain (green and red arrowheads). Mislocalized Crb in the lateral domain (green arrowheads) does not overlap with the elongated SJ region (cyan arrows). (B,B′) Crb overexpression causes punctate/spotlike E-Cad signals in the AJ region (green arrows). Note the mislocalized SAS (red arrows) and the elongated Cora signals (cyan arrows). (C,C′) Crb-overexpressing SGs have a nearly intact Ndg-positive ECM sheet surrounding the tissue (red arrows). Scale bars: 10 μm.

Development (2014) 141, 1950-1960 doi:10.1242/dev.104166

(Fig. 5E), based on a nearly complete overlap in SJ marker and α-Spec staining (supplementary material Fig. S5). Indeed, TEM analysis revealed rounded basal surfaces and wider spaces between neighboring cells in Cad99C-FL and Cad99CΔCyt-overexpressing SG cells than in wild type, indicating a loss of cell-cell contact, nearly everywhere except where the SJ proteins presumably localize (Fig. 5F). By contrast, most Crb-overexpressing SG cells maintained tight contacts with their neighbors along the entire lateral domain (Figs 4F and 6A), perhaps through homophilic adhesion between the Crb proteins on neighboring cells (Tanentzapf et al., 2000). These data support the idea that Cad99C does not mediate homophilic adhesion (D'Alterio et al., 2005) and suggest that membrane accumulation of Cad99C specifically disfavors cell-cell contact, leading to cell rounding.

The morphological changes in the basolateral domain of SG cells also correlated with changes in ECM organization, based on localization of Nidogen (Ndg), a glycoprotein with important linker functions in basement membranes (Hynes and Zhao, 2000). In *Drosophila*, Ndg-positive ECM, which is deposited by a subset of mesodermal cells (Broadie et al., 2011), is detected in thin sheets attached to the surface of many internal organs (Wolfstetter and Holz, 2012), with noticeable intensity around SGs at later stages of development (Fig. 5G). Compared with the strong Ndg localization surrounding the basal side of wild-type SGs (Fig. 5G), Cad99C-FL- or Cad99CΔCyt-expressing SGs with rounded basal domains showed only trace amounts of Ndg staining (Fig. 5H; data not shown). Notably, Crb-overexpressing SGs had largely intact Ndg-positive ECM structures surrounding the tissue (Fig. 6C).

### SAS expression also affects cell and ECM architecture

As the 'converted' apical Cad99C domains always had mislocalized SAS, we asked whether SAS was required for conferring apical character by Cad99C expression. SGs in embryos missing either *sas* alone or missing both *sas* and zygotic *Cad99C* were largely normal (data not shown). Overexpression of Cad99CΔCyt in an *sas*-null background (transheterozygotes of *sas* protein null mutant and deficiency) showed the same SG phenotype as in a wild-type background (Fig. 7A), suggesting that the Cad99C overexpression phenotypes are independent of SAS. Surprisingly, SAS overexpression also expanded apical membranes (Fig. 7B,C). TEM analysis revealed both increased microvilli-like apical structures and apical membrane expansion into the lateral domain (Fig. 7E). E-Cad staining was somewhat reduced and irregular in the AJ domain, and was increased in basolateral domains in the full-length SAS (SAS-FL)-overexpressing SG cells, except in the SJ domain (Fig. 7C; data not shown). SAS-FL overexpression with a stronger line caused more severe morphological defects with rounded cells that correlated with mislocalized basal SAS (Fig. 7D). Very strong F-actin signals were observed in the apical membranes that extended into the lateral domain (Fig. 7D) and elongated SJ domains were observed in regions devoid of SAS (Fig. 7D), reminiscent of both Cad99C- and Crb-overexpression phenotypes. The SAS-mislocalized domain did not stain with antibodies to Cad99C or Crb (data not shown), suggesting that all three proteins are capable of 'apicalizing' membrane independently. As with Cad99C, overexpressed SAS-FL signals colocalized with Rab6 (Fig. 7F).

SAS contains several motifs involved in protein-protein interaction, including von Willebrand factor (vWF) type C domains and fibronectin type 3 (FN3) domains in its large extracellular domain; no known functional motifs have been discovered, however, in the small cytoplasmic domain (consisting of only 37 residues). Overexpressed SASΔCyt (entire cytoplasmic region deleted) localized apically and almost completely phenocopied the SAS-FL overexpression phenotypes (supplementary material Fig. S6). Interestingly, SASΔCyt-overexpressing SG cells have Crb dispersed

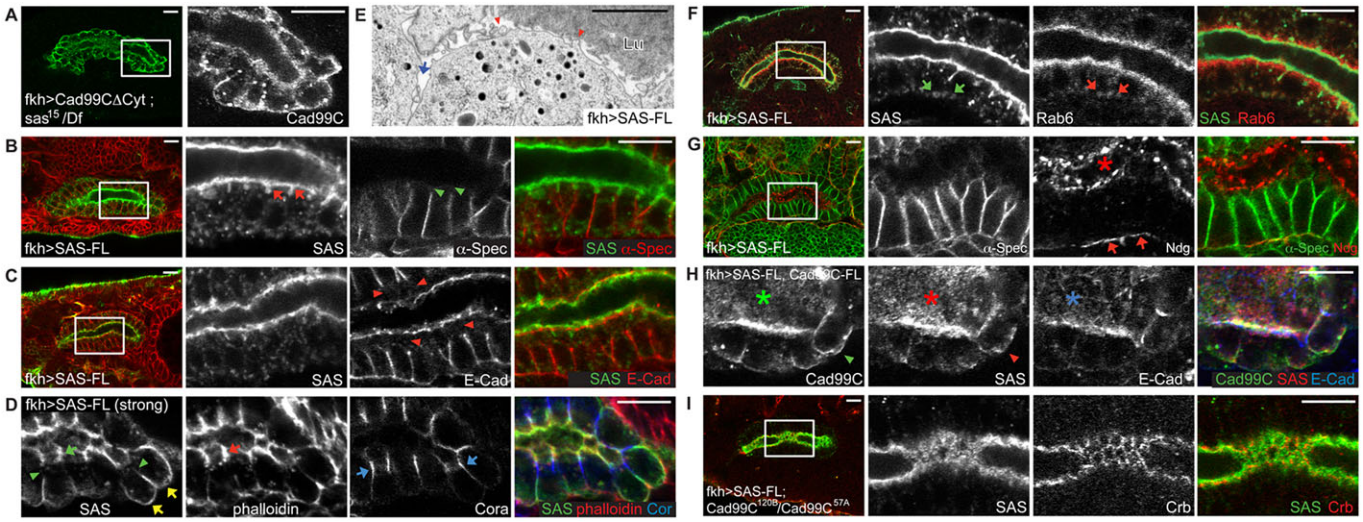


**Fig. 7. SAS overexpression causes similar, but distinct, phenotypes to those of Cad99C-overexpression.** (A-D,F-I) Single sections of confocal images of stage 16 SGs. (A) Cad99CΔCyt overexpression in an *sas* mutant background causes the same phenotypes as it does in a wild-type background. (B) SAS overexpression causes apical membranes to protrude into the lateral domains (red arrows), where the lateral membrane marker α-Spec is absent (green arrowheads). (C) E-Cad signals are absent in the apical region of the lateral domain in SAS-overexpressing SGs (red arrowheads). (D) Overexpression of SAS with a stronger UAS line causes mislocalization of SAS to the basal domain (yellow arrows) and cell rounding. Overexpression of SAS also causes apical membrane expansion into the lateral domain, where strong F-actin signals are found (green and red arrows), as well as over-elongated SJ regions (cyan arrows), where SAS is excluded (green arrowheads). (E) TEM image of SAS-overexpressing stage 16 SG. Note the microvilli-like apical structures (red arrowheads) and the rounder apical surface protruding into the lateral domain (cyan arrow). (F) The punctate signals of overexpressed SAS (green arrows) colocalize with Rab6 (red arrows). (G) SAS-overexpressing SGs have strong Ndg signals (red arrows) in the apical ECM (red asterisk). (H) Co-overexpression of Cad99C-FL and SAS-FL causes huge expansion of apical membranes (green and red asterisks) and rounded cell shapes (green and red arrowheads). E-Cad signals are dispersed throughout the apical domain (cyan asterisk). (I) SAS overexpression in the zygotic *Cad99C* mutant background causes the same phenotype as in wild type. Scale bars: 2 μm in E; 10 μm in others.

Development (2014) 141, 1950-1960 doi:10.1242/dev.104166

along the apical surface, unlike with the SAS-FL-overexpressing cells, where Crb primarily localized to the normal SAR domain (supplementary material Fig. S6B,C).

Unexpectedly, strong Ndg signals were observed not only along the basal boundary but also in the apical ECM of SAS-FL-or SAS-ΔCyt-overexpressing SGs (Fig. 7G; supplementary material Fig. S6E,F). As no changes in *ndg* mRNA levels and/or localization were detected (supplementary material Fig. S7), these data suggest abnormal ECM protein turnover in SAS-overexpressing SGs. Moreover, apical Ndg was never observed with overexpression of Cad99C or Crb, suggesting that this is unique to SAS. Co-overexpression of Cad99C-FL and SAS-FL resulted in substantial expansion of apical membranes at the expense of AJ regions, indicated by the dispersed E-Cad signals (Fig. 7H), suggesting additive effects. Loss of *Cad99C* did not affect the SAS-FL overexpression phenotype, further supporting the idea that Cad99C and SAS expand apical membranes independently of each other (Fig. 7I).

Altogether, these studies reveal that two apical surface transmembrane proteins – Cad99C and SAS – can confer apical properties to other membrane domains. These properties include a loss of cell-cell contact, ectopic accumulation of apical markers with a corresponding loss of the junctional markers that are characteristic of lateral domains, as well as changes in the distribution of ECM markers that are characteristic of basal domains. Our studies also suggest that the SJ, the site where known basolateral determinants are found, is the membrane domain most refractory to apical conversion.

## DISCUSSION

Here, we describe previously undiscovered roles for apical surface proteins in regulating apical membranes and impacting overall tissue architecture in *Drosophila* tubular epithelia. As loss and overexpression of Cad99C affect cell rearrangement during tube elongation and as the apical ECM is also partially disrupted in the Cad99C-overexpressing SGs, we propose that adhesion between the apical cell surface and apical ECM affects cell rearrangement in *Drosophila* SGs (Fig. 8). We propose that the adhesion between the apical surface and apical ECM through Cad99C serves to counteract the as yet un-described forces driving the cell rearrangement events that elongate the SG tube. With loss of *Cad99C*, adhesion is weakened, allowing cells to rearrange more easily, resulting in longer SGs with fewer cells surrounding the tube circumference. Correspondingly, too much Cad99C increases adhesion, making it more difficult for tubes to elongate by cell rearrangement, resulting in wider glands with more cells surrounding the tube circumference. Normal cell rearrangement with Cad99CΔCyt overexpression (the same number of cells in cross section as WT) suggests a role for the cytoplasmic domain in this process. Supporting the role for Cad99C in adhesion between the apical surface and the apical ECM, Cad99C loss significantly rescues the irregular apical membrane phenotype observed in SGs mutant for the secreted AdamTS-A metalloprotease (Ismat et al., 2013). Interactions between the apical ECM and membrane-spanning apical cell surface proteins have also been suggested from studies of the roles of zona pellucida (ZP) domain-containing proteins in *Drosophila* tracheal development (Bökel et al., 2005; Jaźwińska et al., 2003); loss of these proteins can lead to a complete loss of connections between tracheal cells undergoing tube elongation by cell rearrangement.

Overexpression of Cad99C regulates total apical area, consistent with the function of Cad99C in follicle cells in regulating microvillar length (D'Alterio et al., 2005; Schlichting et al., 2006); the extra membrane associated with Cad99C overexpression in tubular epithelia, however, appears in two forms: microvilli-like projections and expansion of the apical surface into the lateral domain, apparently at the expense of apical lateral structures, such as AJs (Fig. 8).

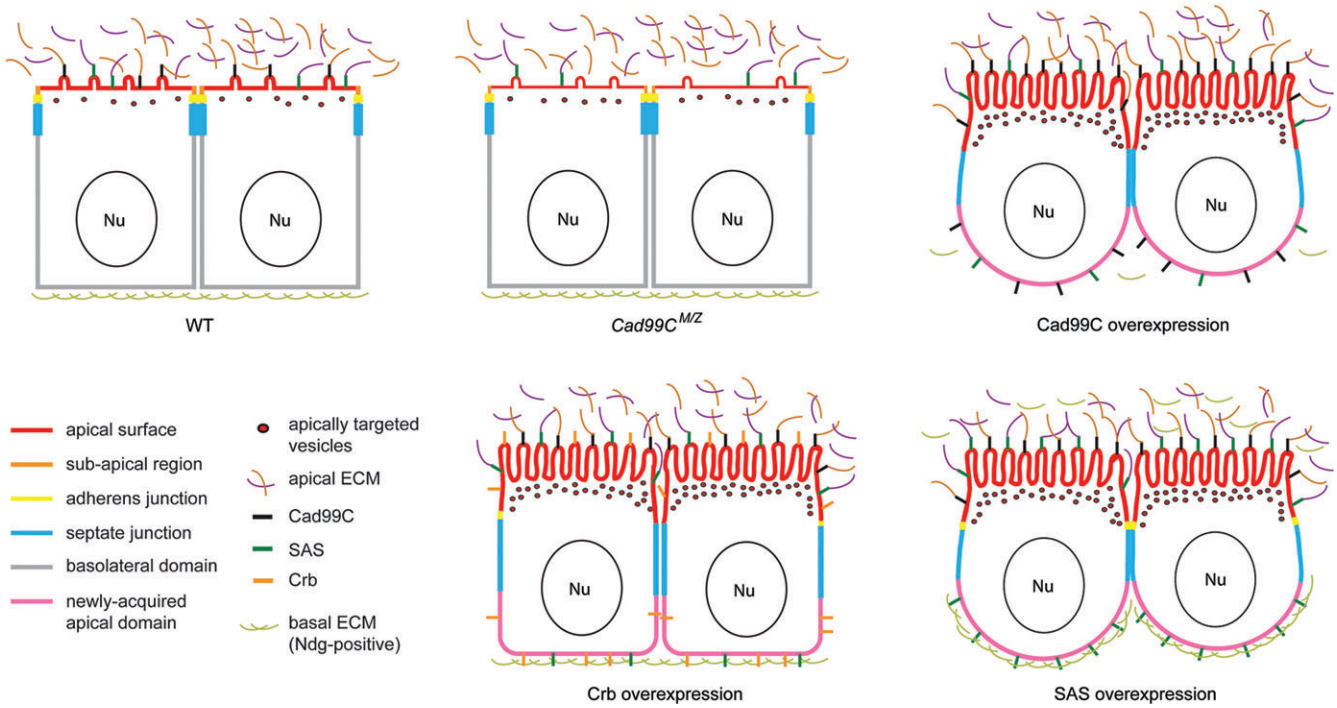


**Fig. 8. A model for how apical surface proteins affect apical membranes in tubular epithelia.** Cad99C and SAS bind to as yet unidentified apical ECM proteins on the apical surface. This binding adheres the gland to the apical ECM. Changes in adhesion by loss or overexpression of Cad99C affect the rearrangement of SG cells during tube elongation. Overexpression of Cad99C/Crb/SAS causes apical membrane expansion that results in changes in cell architecture, but only Cad99C and SAS overexpression affect basal ECM structure or distribution.

Development (2014) 141, 1950-1960 doi:10.1242/dev.104166

Interestingly, SAS also drives apical area expansion when overexpressed, causing both increases in microvilli and expansion into the lateral domain.

Several lines of evidence suggest that Cad99C and SAS, like Crb, drive apical conversion in tubular epithelia (Fig. 8). First, Cad99C mislocalization always correlates with mislocalization of SAS in the same domain. Second, the actin cytoskeleton is reorganized. Strong F-actin signals are characteristic of the apical domain, and F-actin is much more enriched in the Cad99C- or SAS-mislocalized basal domain than in wild-type cells. Third, the Cad99C- and SAS-mislocalized domains are mutually exclusive with the remaining lateral domains, where SJ proteins localize. The elongated SJ protein distribution could be due to the SJ structures being disrupted because a dye exclusion assay revealed compromised barrier function in the completely rounded Cad99C- or SAS-overexpressing SG cells (data not shown) and because mislocalization of SJ proteins into the entire basolateral domain has been reported in many SJ mutants (Laval et al., 2008; Nelson et al., 2010; Paul et al., 2003; Wu et al., 2004). Alternatively, the elongated SJs could be due to cells establishing new SJ domains in more basolateral regions in response to the new apical domains being established nearby.

The cell rounding caused by Cad99C and SAS mislocalization probably reflects the loss of cell-cell adhesion, which we suspect normally imposes the columnar/cuboidal shapes on epithelial cells. Indeed, one feature of the apical surface is favoring cell-matrix over cell-cell contact. Moreover, the loss of basal ECM (Ndg) observed with Cad99C overexpression also suggests a loss of basal character; the cells either no longer properly localize the basal proteins that bind Ndg and/or other basal ECM components or the basally localized Cad99C somehow interferes with this binding. The abnormal Ndg localization to both apical and basal surfaces in SAS-overexpressing SGs supports some level of basal ECM internalization (Godyna et al., 1995; Memmo and McKeown-Longo, 1998; Wienke et al., 2003) and recycling to the membrane, given that SG cells do not synthesize this protein (supplementary material Fig. S7). Indeed, co-overexpression of Cad99CΔCyt and SAS results in a complete loss of Ndg staining in the region of the SG (data not shown). The differential effects of Cad99C and SAS on Ndg accumulation suggest unique activities for each protein in establishing/maintaining the apical surface. Cad99C and SAS may have a common role in binding to and organizing the apical ECM, but the exact components they bind both inside and outside the cell are likely to be distinct.

Our finding that two apical membrane components – Cad99C and SAS – can confer apical character on other membrane domains suggests that multiple avenues exist for establishing and/or maintaining overall epithelial polarity. Learning how these and the previously known determinants function should provide new insight into the contributions of cell-cell and cell-matrix interactions towards specifying polarized membrane domains. Importantly, our findings on the role of Cad99C in apical membrane expansion – potentially mediated through interactions with the apical ECM – may provide additional insight into how mutations in the human Usher proteins contribute to progressive sensory loss.

## MATERIALS AND METHODS

### Flies and antibodies

Fly strains used in this study were: *Oregon R*; *Cad99C*$^{57A}$, *Cad99C*$^{120B}$, *UAS-Cad99C-FL-GFP*, *UAS-Cad99CΔCyt, UAS-Cad99CΔEx* (Schlichting et al., 2006); *UAS-Cad99C-FL, UAS-Cad99CΔCyt-31-GFP* (D'Alterio et al., 2005); *fkh-Gal4* (Henderson and Andrew, 2000); *btl*-Gal4 (Shiga et al., 1996); *ubi-RFP-Rab6* (Januschke et al., 2007); *UAS PLCδ-PH-GFP* (von Stein et al., 2005); and *sas*$^{15}$ (Lewis et al., 1980; Lee et al., 2013).

To generate the *UAS-Cad99CΔPBD* transgenic flies, the Cad99C open reading frame (ORF) deleting the putative PDZ-binding domains [nine amino acid residues (SEVETTTEL) from the C-terminal region of Cad99C, underlined residues indicate consensus of Class I PDZ domain-binding sites] was amplified using the UAS-Cad99C-FL genomic DNA as a template. To generate the UAS-SAS-FL and UAS-SASΔCyt transgenic flies, the entire SAS ORF and the fragment deleting the cytoplasmic domain (37 amino acids) were amplified, respectively, using LD44801 EST clone as a template. The constructs were subcloned into the pUAST vector (Brand and Perrimon, 1993) using the Gateway system (Carnegie Institution).

Primary antibodies included anti-β-gal (Promega, 1:500), anti-GFP (Molecular Probes, 1:10,000), rabbit anti-Cad99C (Cad99C-RB; peptide antibody specific for the C terminus of the Cad99C protein; C. Dahmann, Max Planck Institute of Molecular Cell Biology and Genetics, Germany; 1:3000), guinea pig anti-Cad99C (Cad99C-GP; polyclonal antibody specific for the extracellular region of the Cad99C protein; D. Godt, University of Toronto, Canada; 1:3000), rat α-Cad99C (Cad99C-RT; polyclonal antibody specific for the intracellular region of the Cad99C protein; D. Godt; 1:25), anti-Crb (DSHB, 1:10), anti-SAS (D. Cavener, Penn State University, PA, USA; 1:500), anti-α-Spec (DSHB, 1:1), anti-aPKC (Santa Cruz, 1:200), anti-$\beta_H$-spectrin (G. Thomas, Pennsylvania State University, USA; 1:100), anti-DE-Cad (DSHB, 1:10), anti-Arm (DSHB, 1:100), anti-Cora (R. Fehon, University of Chicago, IL, USA; 1:2000), anti-NrxIV (H. Bellen, Baylor College of Medicine, Houston, TX, USA; 1:2000), anti-Dlg (DSHB, 1:500), anti-Rab11 (S.C. and D.J.A., unpublished) and anti-Ndg (A. Holz, Institut für Allgemeine und Spezielle Zoologie, Germany; 1:2500). Fluorescence-labeled secondary antibodies were used at a 1:500 dilution (Invitrogen). Phalloidin-546 was used at a 1:250 dilution (Invitrogen).

### Immunohistochemistry

Embryo were fixed and stained following standard protocols, except for the α-E-Cad and α-Arm stainings, for which embryos were fixed in 4% paraformaldehyde in PBS and devitellinized with ethanol. For phalloidin staining, embryos were fixed in 1:1 formaldehyde:heptane for 40 min and hand devitellinized. All confocal images were obtained with Zeiss LSM 510. Super-resolution images were obtained with Zeiss ELYRA SR-SIM.

### Whole mount *in situ* hybridization on embryos

*In situ* hybridization was performed as described previously (Lehmann and Tautz, 1994). LD23052 cDNA (DGRC) was used to generate an anti-sense digoxigenin-labeled *Cad99C* RNA probe. An anti-sense RNA probe for *ndg* was made using a PCR fragment (nucleotides 1383-3046) obtained by reverse transcriptase PCR (RT-PCR). cDNAs were made from the total RNAs isolated with TRIzol (Invitrogen) from wild-type embryos.

### Morphometric analyses

Stage 16 SGs were used for analyses in all cases, except for the SG luminal length measurement shown in Fig. 2B, where SGs of both stage 15 and 16 were measured. *Cad99C*$^{120B}$/*Cad99C*$^{57A}$ (*M/Z*) and *Cad99C*$^{57A}$/*Cad99C*$^{120B}$ (*M/Z*) mutants are the progeny from crossing homozygous *Cad99C*$^{120B}$ females and homozygous *Cad99C*$^{57A}$ males, and from crossing homozygous *Cad99C*$^{57A}$ females and homozygous *Cad99C*$^{120B}$ males, respectively. Maternal mutants *Cad99C*$^{120B}$/+ (*M*) and *Cad99C*$^{57A}$/+ (*M*) are the progeny from crossing homozygous *Cad99C*$^{120B}$ and homozygous *Cad99C*$^{57A}$ females to wild-type males, respectively. *Cad99C*$^{57A}$/*Cad99C*$^{120B}$ and *Cad99C*$^{120B}$/*Cad99C*$^{57A}$ zygotic mutants are the progeny from crossing heterozygous parents. The images of stage 15 and stage 16 embryos (Crb staining) from perfect ventral views were taken with ProgRes C14*plus* camera (Jenoptik). The middle of the SG lumen was traced using the Image J program (NIH). For quantification shown in Fig. 4F, lateral views of the projected confocal images of wild-type, Cad99C-FL- and Cad99CΔCyt-overexpressing SGs (SAS staining) were used.

To measure the luminal area, confocal images of Crb or SAS staining were projected to visualize the entire lumen. The luminal area was traced and calculated using ImageJ. To measure the apical domain size of individual SG cells, confocal images of E-Cad staining were traced and measured using

ImageJ. The elongation ratio of the same cells was determined by calculating the ratio of apical domain length oriented along the proximal-distal (PD) axis to the apical domain length along the dorsal-ventral (DV) axis passing the centeroid of each cell. Statistical significance was calculated using Student's *t*-test (two-tailed).

### Quantification of the number of the nuclei per cross-section of SGs

Wild-type, $Cad99C^{120B}/Cad99C^{57A}$ (*M/Z*), *fkh>Cad99C-FL* and *fkh>Cad99CΔCyt* embryos were stained for membrane markers and with DAPI. Cross-sections of confocal images of SGs were obtained with the Zeiss LSM 510 program. Nuclei were counted in three independent cross-sections per SG and averaged. Statistical significance was calculated using Student's *t*-test (two-tailed).

### High pressure freezing/freeze substitution transmission electron microscopy

Dechorionated embryos were high pressure frozen with the Leica EM HPM 100, in 200 µm aluminum specimen carriers filled with yeast paste containing 10% methanol (McDonald and Morphew, 1993). Samples were then freeze substituted in a fixing cocktail containing 1% osmium, 0.1% uranyl acetate, 95% acetone and 5% water for better preservation of membranes (Walther and Ziegler, 2002). The freeze substitution was performed in a Leica EM AFS 2/FSP with a modified schedule (correspondence Rick Fetter, Janelia Farms HHMI). Samples were gradually infiltrated with 33%/50%/75% increasing Eponate 12 (Pella) mixture in acetone, with a pure resin infiltration overnight, and cured at 60°C for 2 days. Sections (60 nm) were stained with 1% tannic acid followed by 2% uranyl acetate and 0.3% lead citrate. Grids were viewed on a Phillips CM120 Transmission Electron Microscope and digital images captured with an ER-80 AMT 8 megapixel CCD camera. Sections from at least four independent embryos were analyzed for wild type and *fkh-Gal4>Cad99C-FL*, and from two embryos for $Cad99C^{M/Z}$, *fkh-Gal4>Cad99CΔCyt* and *fkh-Gal4>SAS-FL*.

#### Acknowledgements

We thank C. Dahmann, D. Godt, D. Cavener, R. Fehon, H. Bellen, A. Holz, G. Thomas, the Bloomington Stock Center and Drosophila Genomics Resource Center for providing fly stocks, antibodies or cDNAs used in this study. We thank FlyBase for information on the genes used in this study (St Pierre et al., 2014). We also thank M. Delannoy and B. Smith of the microscope facility in the Johns Hopkins University School of Medicine for technical assistance for TEM analysis. In addition, we thank members of the Andrew laboratory, and A. Ewald, A. Hubbard, G. Seydoux and three anonymous reviewers for their comments on this manuscript.

#### Competing interests

The authors declare no competing financial interests.

#### Author contributions

S.C. and D.J.A. designed the experiments, analyzed the data, and wrote the paper. S.C. performed the experiments.

#### Funding

This work was supported by the National Institutes of Health (NIH) [K99 DE021068 to S.C. and RO1 DE013899 to D.J.A.]. The HPF/AFS used for preparing the TEM samples was acquired with NIH grant S10RR026445. Deposited in PMC for release after 12 months.

#### Supplementary material

Supplementary material available online at http://dev.biologists.org/lookup/suppl/doi:10.1242/dev.104166/-/DC1

#### References

**Baumgartner, S., Littleton, J. T., Broadie, K., Bhat, M. A., Harbecke, R., Lengyel, J. A., Chiquet-Ehrismann, R., Prokop, A. and Bellen, H. J.** (1996). A Drosophila neurexin is required for septate junction and blood-nerve barrier formation and function. *Cell* **87**, 1059-1068.

**Bilder, D. and Perrimon, N.** (2000). Localization of apical epithelial determinants by the basolateral PDZ protein Scribble. *Nature* **403**, 676-680.

**Bökel, C., Prokop, A. and Brown, N. H.** (2005). Papillote and Piopio: drosophila ZP-domain proteins required for cell adhesion to the apical extracellular matrix and microtubule organization. *J. Cell Sci.* **118**, 633-642.

**Brand, A. H. and Perrimon, N.** (1993). Targeted gene expression as a means of altering cell fates and generating dominant phenotypes. *Development* **118**, 401-415.

**Broadie, K., Baumgartner, S. and Prokop, A.** (2011). Extracellular matrix and its receptors in Drosophila neural development. *Dev. Neurobiol.* **71**, 1102-1130.

**Coutelis, J.-B. and Ephrussi, A.** (2007). Rab6 mediates membrane organization and determinant localization during Drosophila oogenesis. *Development* **134**, 1419-1430.

**D'Alterio, C., Tran, D. D. D., Au Yeung, M. W. Y., Hwang, M. S. H., Li, M. A., Arana, C. J., Mulligan, V. K., Kubesh, M., Sharma, P., Chase, M. et al.** (2005). Drosophila melanogaster Cad99C, the orthologue of human Usher cadherin PCDH15, regulates the length of microvilli. *J. Cell Biol.* **171**, 549-558.

**Del Nery, E., Miserey-Lenkei, S., Falguières, T., Nizak, C., Johannes, L., Perez, F. and Goud, B.** (2006). Rab6A and Rab6A' GTPases play non-overlapping roles in membrane trafficking. *Traffic* **7**, 394-407.

**Godyna, S., Liau, G., Popa, I., Stefansson, S. and Argraves, W. S.** (1995). Identification of the low density lipoprotein receptor-related protein (LRP) as an endocytic receptor for thrombospondin-1. *J. Cell Biol.* **129**, 1403-1410.

**Henderson, K. D. and Andrew, D. J.** (2000). Regulation and function of Scr, exd, and hth in the Drosophila salivary gland. *Dev. Biol.* **217**, 362-374.

**Hynes, R. O. and Zhao, Q.** (2000). The evolution of cell adhesion. *J. Cell Biol.* **150**, F89-F96.

**Ismat, A., Cheshire, A. M. and Andrew, D. J.** (2013). The secreted AdamTS-A metalloprotease is required for collective cell migration. *Development* **140**, 1981-1993.

**Januschke, J., Nicolas, E., Compagnon, J., Formstecher, E., Goud, B. and Guichet, A.** (2007). Rab6 and the secretory pathway affect oocyte polarity in Drosophila. *Development* **134**, 3419-3425.

**Jaźwińska, A., Ribeiro, C. and Affolter, M.** (2003). Epithelial tube morphogenesis during Drosophila tracheal development requires Piopio, a luminal ZP protein. *Nat. Cell Biol.* **5**, 895-901.

**Kerman, B. E., Cheshire, A. M., Myat, M. M. and Andrew, D. J.** (2008). Ribbon modulates apical membrane during tube elongation through Crumbs and Moesin. *Dev. Biol.* **320**, 278-288.

**Lamb, R. S., Ward, R. E., Schweizer, L. and Fehon, R. G.** (1998). Drosophila coracle, a member of the protein 4.1 superfamily, has essential structural functions in the septate junctions and developmental functions in embryonic and adult epithelial cells. *Mol. Biol. Cell* **9**, 3505-3519.

**Laprise, P. and Tepass, U.** (2011). Novel insights into epithelial polarity proteins in Drosophila. *Trends Cell Biol.* **21**, 401-408.

**Laval, M., Bel, C. and Faivre-Sarrailh, C.** (2008). The lateral mobility of cell adhesion molecules is highly restricted at septate junctions in Drosophila. *BMC Cell Biol.* **9**, 38.

**Lee, H.-K., Cording, A., Vielmetter, J. and Zinn, K.** (2013). Interactions between a receptor tyrosine phosphatase and a cell surface ligand regulate axon guidance and glial-neuronal communication. *Neuron* **78**, 813-826.

**Lehmann, R. and Tautz, D.** (1994). In situ hybridization to RNA. *Methods Cell Biol.* **44**, 575-598.

**Lewis, R., Kaufman, T., Denell, R. and Tallerico, P.** (1980). Genetic analysis of the Antennapedia gene complex (ANT-C) and adjacent chromosomal regions of Drosophila melanogaster. *Genetics* **95**, 367-381.

**Mallard, F., Tang, B. L., Galli, T., Tenza, D., Saint-Pol, A., Yue, X., Antony, C., Hong, W., Goud, B. and Johannes, L.** (2002). Early/recycling endosomes-to-TGN transport involves two SNARE complexes and a Rab6 isoform. *J. Cell Biol.* **156**, 653-664.

**Martinez, O., Schmidt, A., Salaméro, J., Hoflack, B., Roa, M. and Goud, B.** (1994). The small GTP-binding protein rab6 functions in intra-Golgi transport. *J. Cell Biol.* **127**, 1575-1588.

**Martinez, O., Antony, C., Pehau-Arnaudet, G., Berger, E. G., Salamero, J. and Goud, B.** (1997). GTP-bound forms of rab6 induce the redistribution of Golgi proteins into the endoplasmic reticulum. *Proc. Natl. Acad. Sci. U.S.A.* **94**, 1828-1833.

**Maruyama, R. and Andrew, D. J.** (2012). Drosophila as a model for epithelial tube formation. *Dev. Dyn.* **241**, 119-135.

**McDonald, K. L. and Auer, M.** (2006). High-pressure freezing, cellular tomography, and structural cell biology. *Biotechniques* **41**, 137-143.

**McDonald, K. and Morphew, M. K.** (1993). Improved preservation of ultrastructure in difficult-to-fix organisms by high pressure freezing and freeze substitution: I. Drosophila melanogaster and Strongylocentrotus purpuratus embryos. *Microsc. Res. Tech.* **24**, 465-473.

**Memmo, L. M. and McKeown-Longo, P.** (1998). The alpha v beta 5 integrin functions as an endocytic receptor for vitronectin. *J. Cell Sci.* **111**, 425-433.

**Nelson, K. S., Furuse, M. and Beitel, G. J.** (2010). The Drosophila Claudin Kune-kune is required for septate junction organization and tracheal tube size control. *Genetics* **185**, 831-839.

**Opdam, F. J., Echard, A., Croes, H. J., van den Hurk, J. A., van de Vorstenbosch, R. A., Ginsel, L. A., Goud, B. and Fransen, J. A.** (2000). The small GTPase Rab6B, a novel Rab6 subfamily member, is cell-type specifically expressed and localised to the Golgi apparatus. *J. Cell Sci.* **113**, 2725-2735.

**Paul, S. M., Ternet, M., Salvaterra, P. M. and Beitel, G. J.** (2003). The Na+/K+ ATPase is required for septate junction function and epithelial tube-size control in the Drosophila tracheal system. *Development* **130**, 4963-4974.
**Peifer, M., Orsulic, S., Sweeton, D. and Wieschaus, E.** (1993). A role for the Drosophila segment polarity gene armadillo in cell adhesion and cytoskeletal integrity during oogenesis. *Development* **118**, 1191-1207.
**Pelissier, A., Chauvin, J.-P. and Lecuit, T.** (2003). Trafficking through Rab11 endosomes is required for cellularization during Drosophila embryogenesis. *Curr. Biol.* **13**, 1848-1857.
**Rousso, T., Shewan, A. M., Mostov, K. E., Schejter, E. D. and Shilo, B.-Z.** (2013). Apical targeting of the formin Diaphanous in Drosophila tubular epithelia. *Elife* **2**, e00666.
**Saraste, J. and Goud, B.** (2007). Functional symmetry of endomembranes. *Mol. Biol. Cell* **18**, 1430-1436.
**Satoh, A. K., O'Tousa, J. E., Ozaki, K. and Ready, D. F.** (2005). Rab11 mediates post-Golgi trafficking of rhodopsin to the photosensitive apical membrane of Drosophila photoreceptors. *Development* **132**, 1487-1497.
**Schlichting, K., Demontis, F. and Dahmann, C.** (2005). Cadherin Cad99C is regulated by Hedgehog signaling in Drosophila. *Dev. Biol.* **279**, 142-154.
**Schlichting, K., Wilsch-Bräuninger, M., Demontis, F. and Dahmann, C.** (2006). Cadherin Cad99C is required for normal microvilli morphology in Drosophila follicle cells. *J. Cell Sci.* **119**, 1184-1195.
**Schonbaum, C. P., Organ, E. L., Qu, S. and Cavener, D. R.** (1992). The Drosophila melanogaster stranded at second (sas) gene encodes a putative epidermal cell surface receptor required for larval development. *Dev. Biol.* **151**, 431-445.
**Shiga, Y., Tanaka-Matakatsu, M. and Hayashi, S.** (1996). A nuclear GFP/beta-galactosidase fusion protein as a marker for morphogenesis in living Drosophila. *Dev. Growth Differ.* **38**, 99-106.
**St. Johnston, D. and Ahringer, J.** (2010). Cell polarity in eggs and epithelia: parallels and diversity. *Cell* **141**, 757-774.
**St. Pierre, S. E., Ponting, L., Stefancsik, R. and McQuilton, P.**; **the FlyBase Consortium** (2014). FlyBase 102 - advanced approaches to interrogating FlyBase. *Nucleic Acids Res.* **42**, D780-D788.
**Strand, D., Raska, I. and Mechler, B. M.** (1994). The Drosophila lethal(2)giant larvae tumor suppressor protein is a component of the cytoskeleton. *J. Cell Biol.* **127**, 1345-1360.
**Strickland, L. I. and Burgess, D. R.** (2004). Pathways for membrane trafficking during cytokinesis. *Trends Cell Biol.* **14**, 115-118.
**Tanentzapf, G., Smith, C., McGlade, J. and Tepass, U.** (2000). Apical, lateral, and basal polarization cues contribute to the development of the follicular epithelium during Drosophila oogenesis. *J. Cell Biol.* **151**, 891-904.
**Tepass, U.** (1996). Crumbs, a component of the apical membrane, is required for zonula adherens formation in primary epithelia of Drosophila. *Dev. Biol.* **177**, 217-225.
**Tepass, U.** (2012). The apical polarity protein network in Drosophila epithelial cells: regulation of polarity, junctions, morphogenesis, cell growth, and survival. *Annu. Rev. Cell Dev. Biol.* **28**, 655-685.
**von Stein, W., Ramrath, A., Grimm, A., Müller-Borg, M. and Wodarz, A.** (2005). Direct association of Bazooka/PAR-3 with the lipid phosphatase PTEN reveals a link between the PAR/aPKC complex and phosphoinositide signaling. *Development* **132**, 1675-1686.
**Walther, P. and Ziegler, A.** (2002). Freeze substitution of high-pressure frozen samples: the visibility of biological membranes is improved when the substitution medium contains water. *J. Microsc.* **208**, 3-10.
**Wienke, D., MacFadyen, J. R. and Isacke, C. M.** (2003). Identification and characterization of the endocytic transmembrane glycoprotein Endo180 as a novel collagen receptor. *Mol. Biol. Cell* **14**, 3592-3604.
**Wodarz, A., Hinz, U., Engelbert, M. and Knust, E.** (1995). Expression of crumbs confers apical character on plasma membrane domains of ectodermal epithelia of Drosophila. *Cell* **82**, 67-76.
**Wodarz, A., Ramrath, A., Grimm, A. and Knust, E.** (2000). Drosophila atypical protein kinase C associates with Bazooka and controls polarity of epithelia and neuroblasts. *J. Cell Biol.* **150**, 1361-1374.
**Wolfstetter, G. and Holz, A.** (2012). The role of LamininB2 (LanB2) during mesoderm differentiation in Drosophila. *Cell Mol. Life Sci.* **69**, 267-282.
**Woods, D. F. and Bryant, P. J.** (1991). The discs-large tumor suppressor gene of Drosophila encodes a guanylate kinase homolog localized at septate junctions. *Cell* **66**, 451-464.
**Wu, V. M., Schulte, J., Hirschi, A., Tepass, U. and Beitel, G. J.** (2004). Sinuous is a Drosophila claudin required for septate junction organization and epithelial tube size control. *J. Cell Biol.* **164**, 313-323.
**Zhang, L. and Ward, R. E.** (2009). uninflatable encodes a novel ectodermal apical surface protein required for tracheal inflation in Drosophila. *Dev. Biol.* **336**, 201-212.

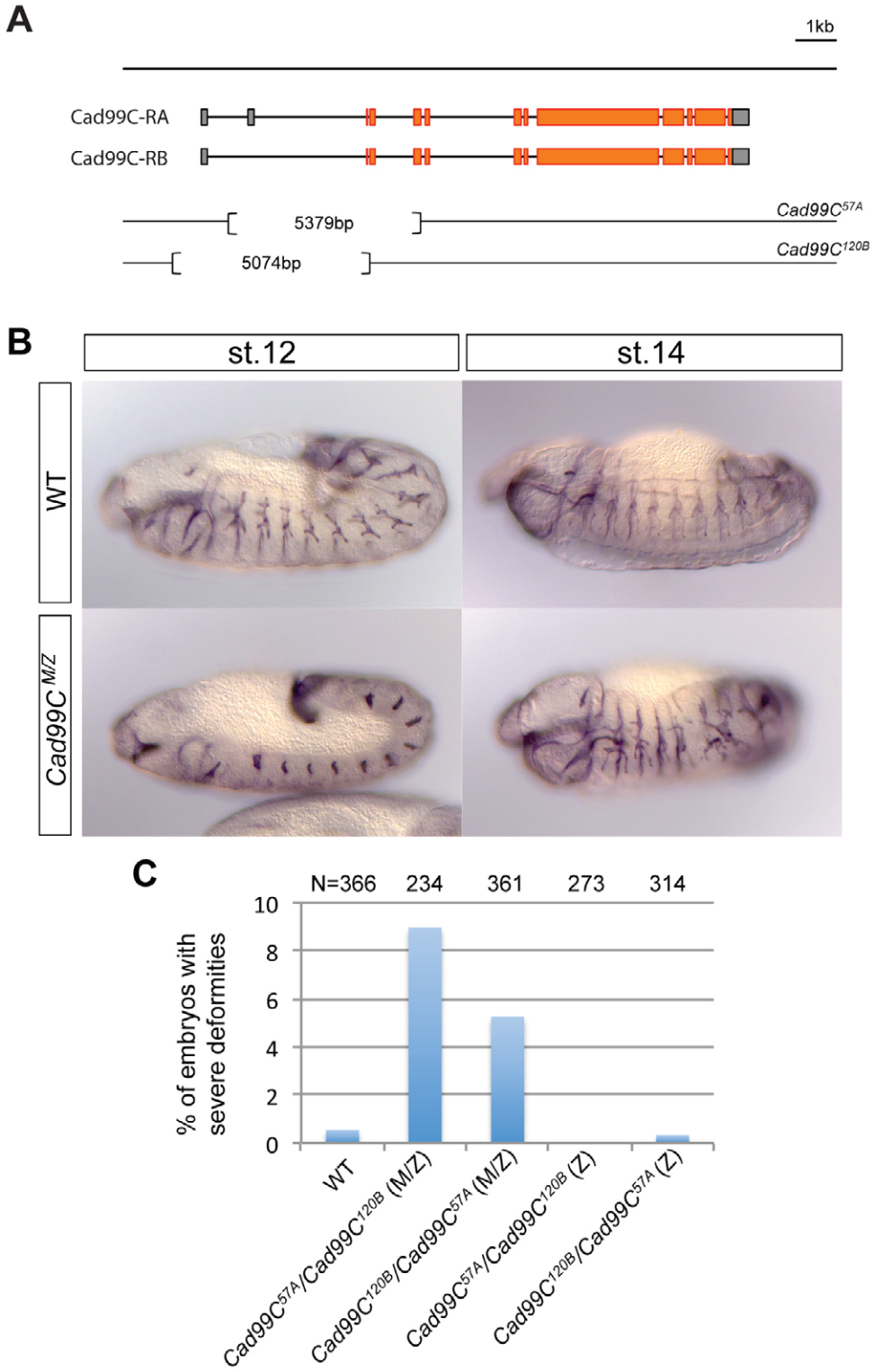


**Fig. S1. Molecular map of the *Cad99C* mutant alleles used in this study.** (A) The gene structure of *Cad99C* and the two alleles used in this study, *Cad99C*$^{57A}$ and *Cad99C*$^{120B}$. The starting codon is deleted in both alleles and both are protein null (Schlichting et al., 2005; Schlichting et al., 2006). The exons encoding the open reading frame are shown in orange. (B) A small subset of the *Cad99C*$^{M/Z}$ embryos that develop have severe morphological defects revealed by staining with Crb. (C) Quantification of the number of *Cad99C*$^{M/Z}$ embryos with severe defects out of the total number that develop is shown.

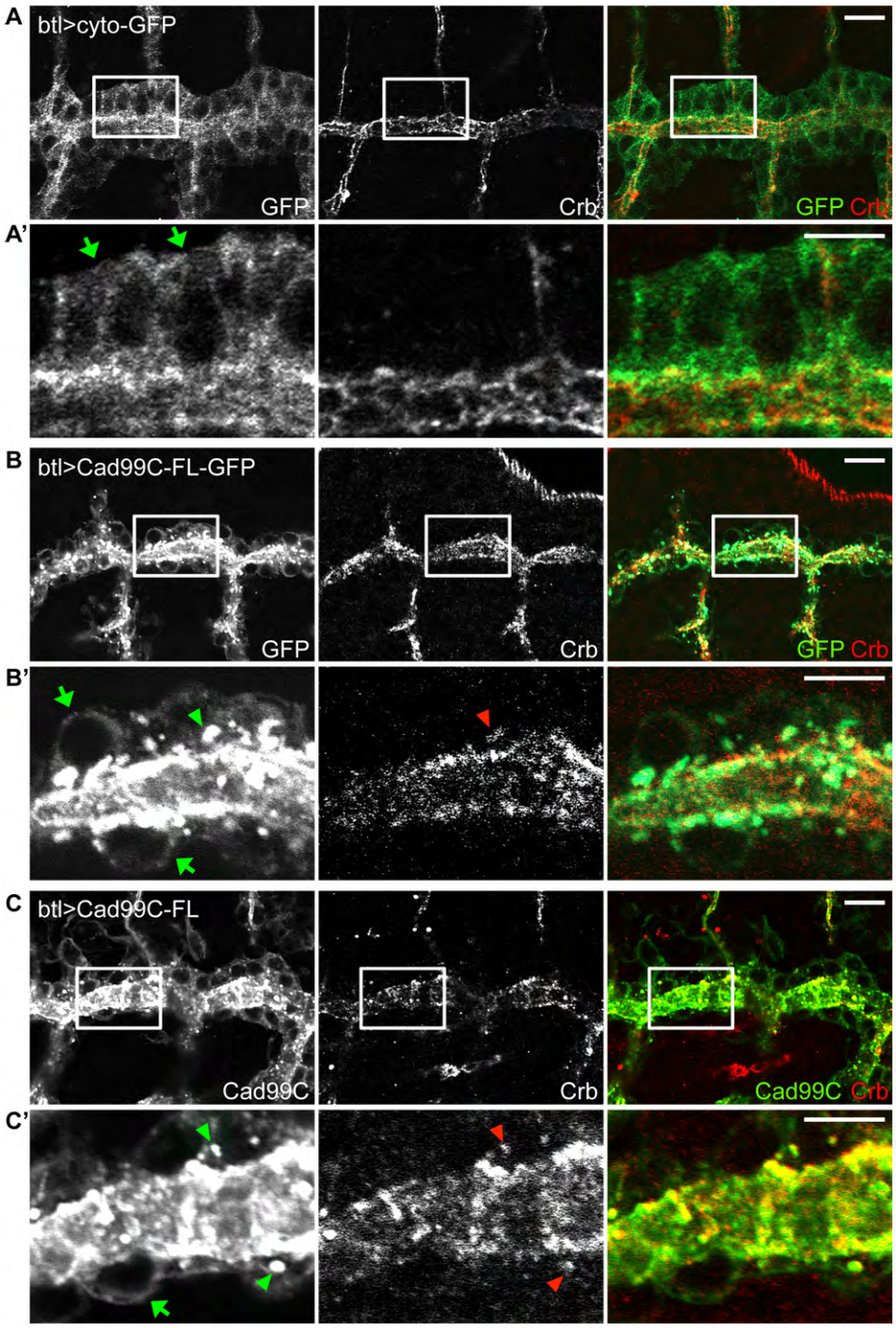


**Fig. S2. Cad99C overexpression in the trachea also results in round epithelial cells.** (A-C) Single sections of confocal images of stage 15 (A, B) and stage 16 trachea (C) (metameres 4-5 in A, C; metameres 3-5 in B). A'-C' are higher magnifications of the boxed regions in A-C. (A) Control embryo is shown expressing cytoplasmic-GFP in tracheal cells under the control of *breathless* (*btl*)-Gal4. Arrows indicate typical cuboidal cell shapes. (B, C) GFP-tagged (B) or untagged (C) Cad99C-FL overexpression in the trachea with *btl*-Gal4 causes expansion of the apical surface and rounding of tracheal cells (green arrows). Crb marks apical membranes (red). Note that Cad99C overexpression resulted in a number of both Cad99C- and Crb-positive large vesicular structures near the apical surface (green and red arrowheads). Scale bars: 10 ㎜.

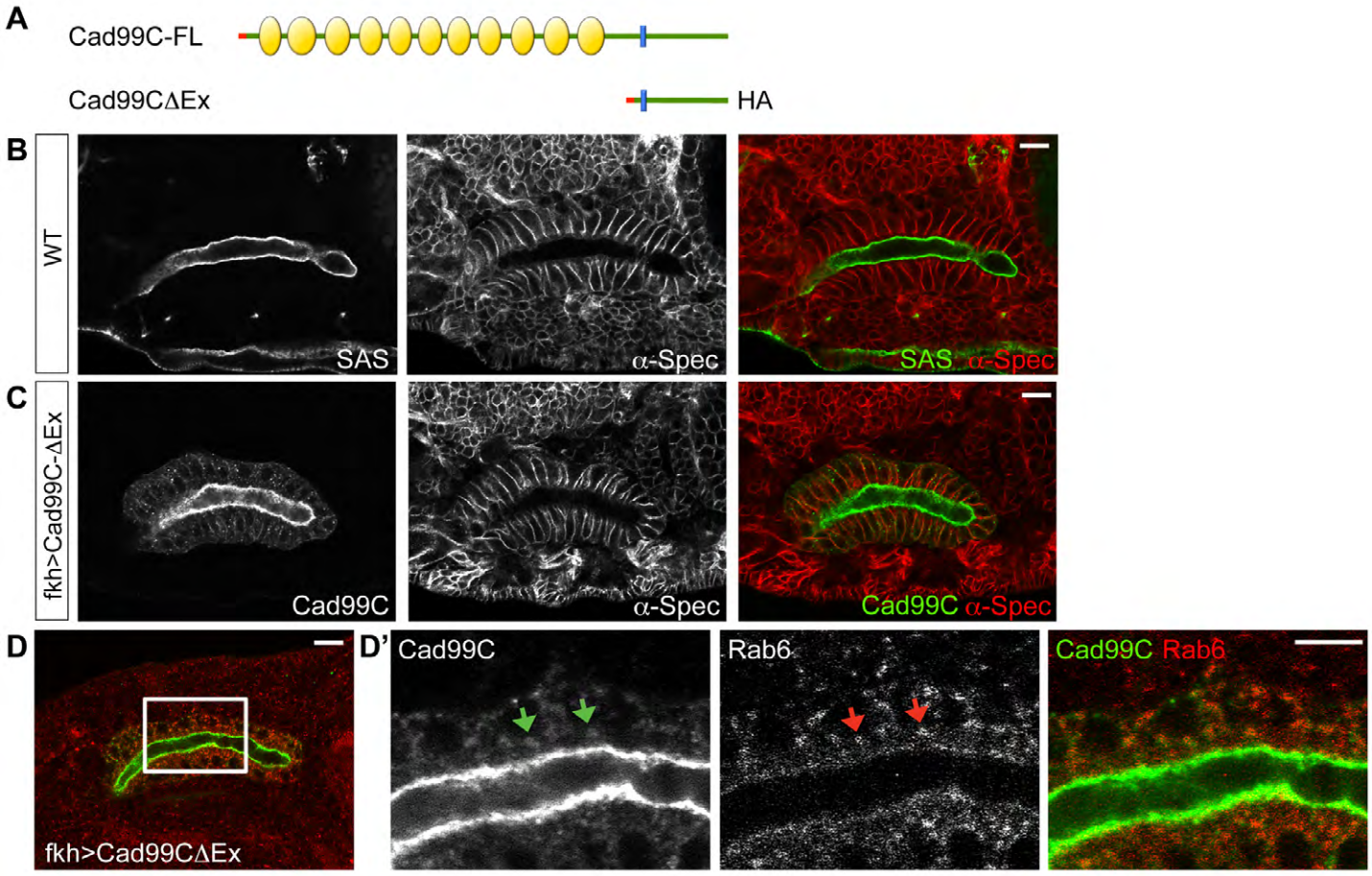


**Fig. S3. Extracellular region-deleted Cad99C does not cause overt phenotypes in tubular organs.** (A) Schematic drawings of full-length (FL) and extracellular region-deleted (ΔEx) Cad99C proteins. The Cad99CΔEx construct has an HA tag at the C terminus. The red bar, the signal peptide; the yellow ovals, the cadherin repeats; the blue rectangle, the transmembrane domain. (B, C) Stage 15 SGs of WT (B) or Cad99CΔEx-HA (C) are morphologically quite similar. Note that Cad99CΔEx protein is mostly detected in the apical membrane, showing similar patterns to SAS in WT and being complimentary to α-Spec, a lateral membrane marker. (D) The cytoplasmic punctate signals of Cad99CΔEx co-localize with Rab6. Scale bars: 10 ㎜.

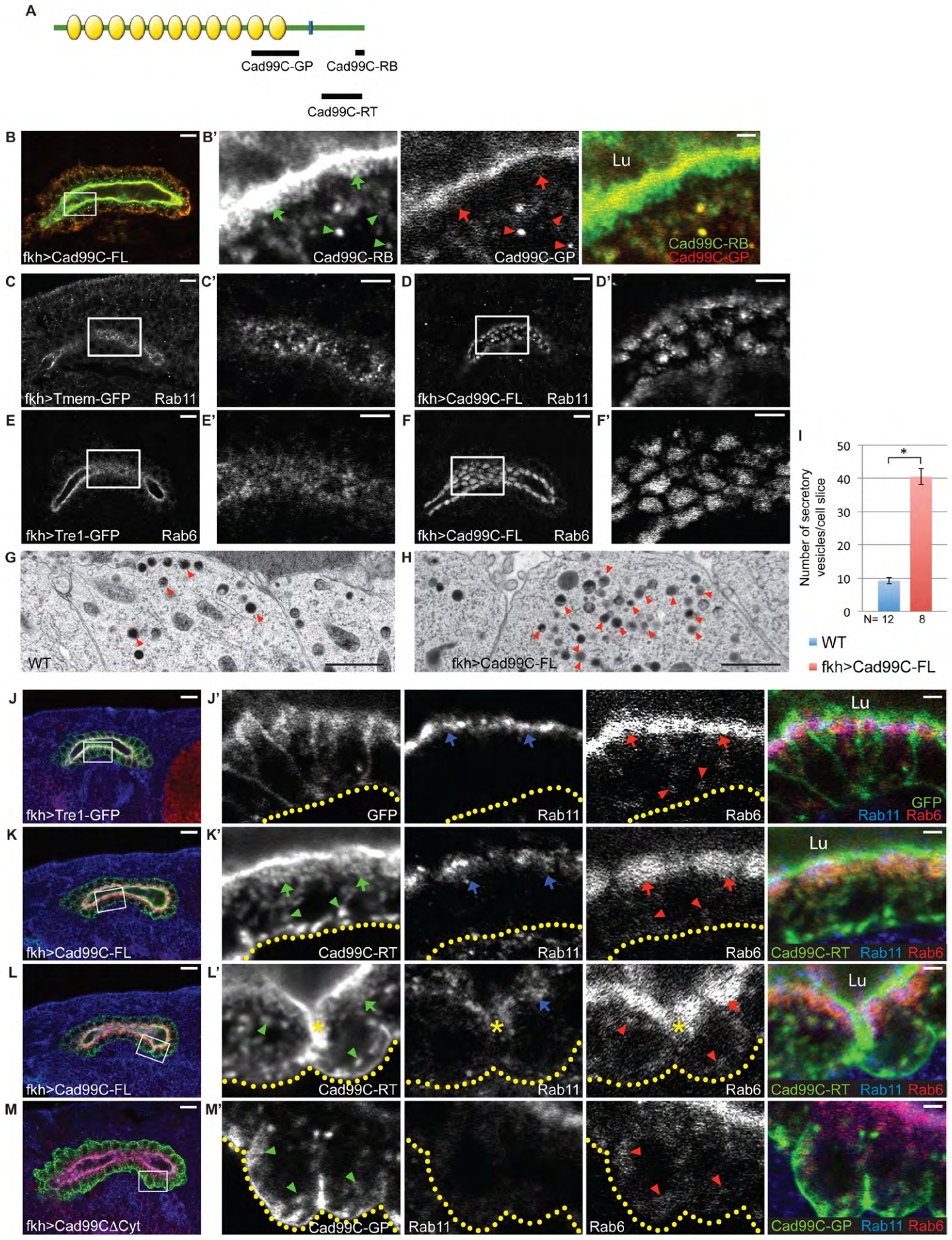
A
Cad99C-GP
Cad99C-RB
Cad99C-RT
B
fkh>Cad99C-FL
B'
Cad99C-RB
Cad99C-GP
Lu
Cad99C-RB
Cad99C-GP
C
fkh>Tmem-GFP
Rab11
C'
D
fkh>Cad99C-FL
Rab11
D'
E
fkh>Tre1-GFP
Rab6
E'
F
fkh>Cad99C-FL
Rab6
F'
G
WT
H
fkh>Cad99C-FL
I
Number of secretory vesicles/cell slice
50
40
30
20
10
0
*
N= 12
8
WT
fkh>Cad99C-FL
J
fkh>Tre1-GFP
J'
GFP
Rab11
Rab6
Lu
GFP
Rab11
Rab6
K
fkh>Cad99C-FL
K'
Cad99C-RT
Rab11
Rab6
Lu
Cad99C-RT
Rab11
Rab6
L
fkh>Cad99C-FL
L'
Cad99C-RT
Rab11
Rab6
Lu
Cad99C-RT
Rab11
Rab6
M
fkh>Cad99CΔCyt
M'
Cad99C-GP
Rab11
Rab6
Cad99C-GP
Rab11
Rab6

**Fig. S4. Vesicular Cad99C co-localizes with Rab6.** (A) A schematic drawing of the Cad99C protein structure shows regions to which antisera were generated indicated with black bars. Yellow oval, cadherin repeats; blue rectangle, the transmembrane domain. (B) A Cad99C-overexpressing SG stained with Cad99C antibodies specific for the intracellular (Cad99C-RB, green) and the extracellular (Cad99C-GP, red) region. B' shows higher magnification of the boxed region. The apical membrane and vesicular structures near the apical membrane are recognized by both Cad99C-RB (green arrows) and Cad99C-GP (red arrows) antibodies, with stronger signals with Cad99C-RB antibody. Cad99C-positive punctate structures are also observed throughout the cells (arrowheads). (C-F) Images of Rab11 or RFP-Rab6 signals in the SGs of control or Cad99C-overexpressing SGs. C'-F' are higher magnifications of C-F. Compared to control glands (C, E), Cad99C-overexpressing SGs have a dramatic increase of Rab11- and Rab6-positive vesicles near the apical surface (D, F). (G, H) TEM analysis shows an increase in the number of apical vesicles in the Cad99C-overexpressing SGs (arrowheads). (I) A histogram of the quantification of the vesicle numbers per cell slice is shown. Error bars: s.e.m. *, $p<10^{-11}$. (J-M) Images of Rab11 (cyan) and RFP-Rab6 (red) signals in the Tre1-GFP, Cad99C-FL or Cad99CΔCyt overexpressing stage 16 SGs (green). K and L are different focal planes of the same gland. J'-M' are higher magnifications of J-M. Rab11-positive vesicles localize in a narrower domain near the apical membrane, both in control (J') and Cad99C-overexpressing SGs (K'-M'). Cad99C-positive vesicular structures overlap more with Rab6-positive vesicles than with Rab11-positive vesicles (arrows in K'-M'). Cad99C-positive punctate structures found throughout the cytoplasm (green arrowheads in K'-M') co-localize with Rab6 signals (red arrowheads in K'-M') but not with Rab11. All confocal images shown here are single sections. Lu, lumen. Scale bars: 10 mm in B-F, J-M and C'-F'; 2 mm in G, H, B', J'-M'.

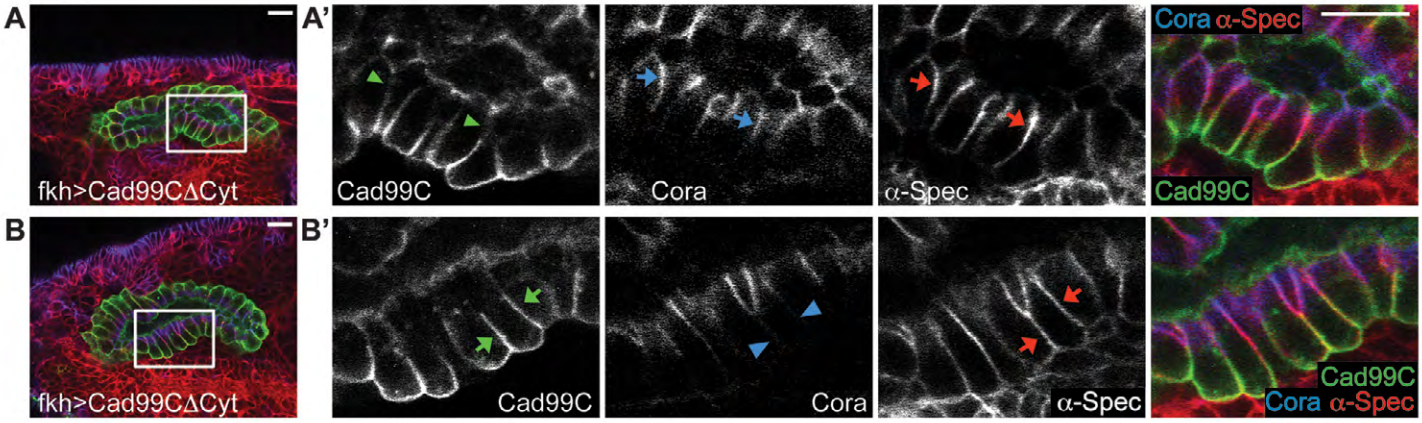


**Fig. S5. Mislocalized Cad99C signals are mutually exclusive with Cora and α-Spec in rounded cells.** (A, B) A single section of a confocal image of stage 16 SG overexpressing Cad99CΔCyt. Higher magnification of the boxed region is shown in A', B'. (A) In many cases, Cora (SJ marker) and α-Spec (lateral membrane marker) show the same localization pattern (cyan and red arrows), which is mutually exclusive with mislocalized Cad99C (green arrowheads). (B) In some cases, however, α-Spec signals overlap mislocalized Cad99C (green and red arrows), where Cora is absent (cyan arrowheads). Scale bars: 10 mm.

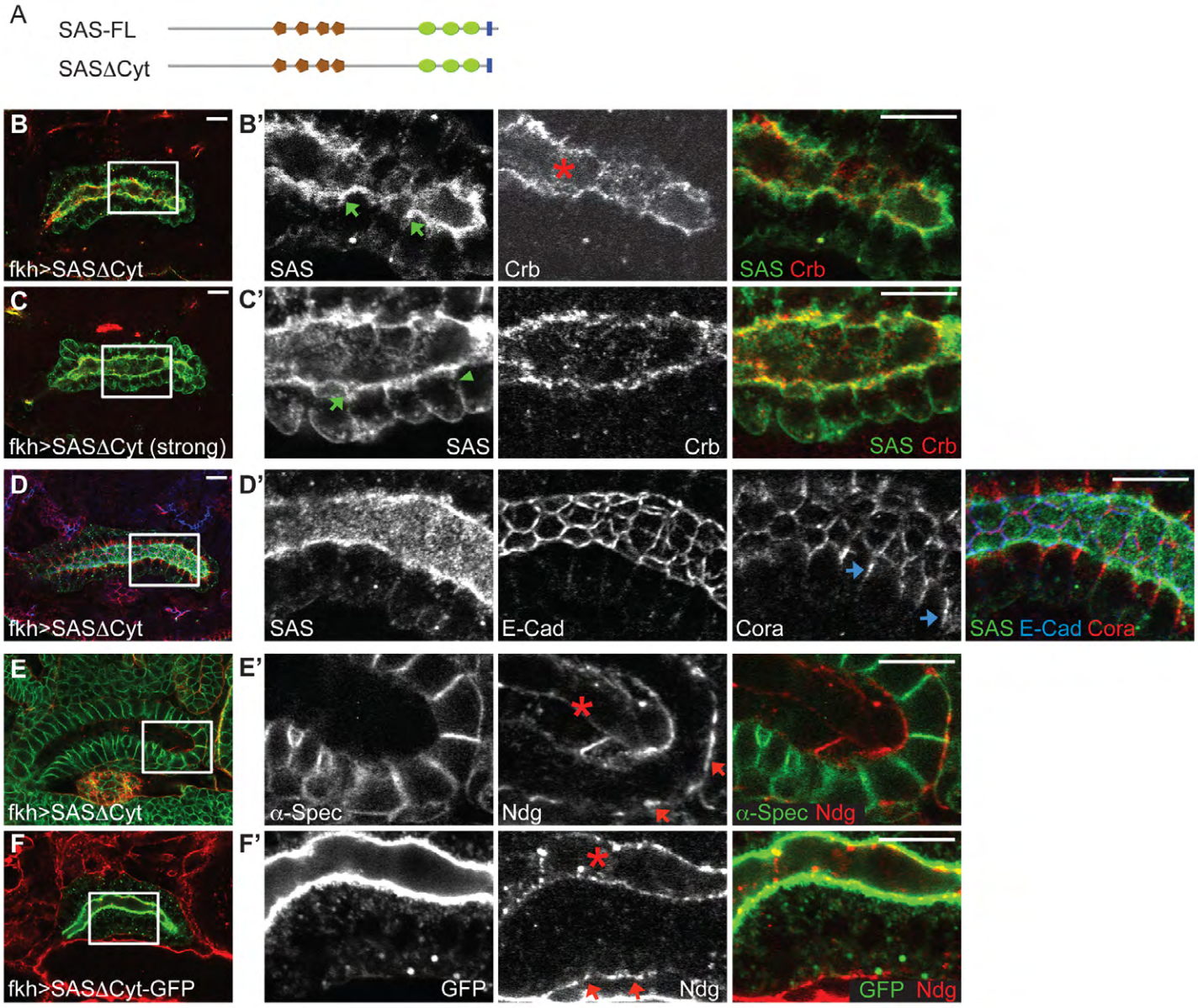


**Fig. S6. SASΔCyt expression almost completely phenocopies SAS-FL overexpression.** (A) Schematic drawings of full-length (FL) and cytoplasmic region-deleted (ΔCyt) SAS proteins. The brown pentagons and the green ovals represent von Willebrand factor (vWF) type C domains and Fibronectin type 3 domains, respectively. The blue rectangle indicates the transmembrane domain. (B) SASΔCyt-overexpressing SGs have expanded apical membranes protruding into the lateral domain (green arrows). Note that the Crb signals are more dispersed and less enriched in the SAR (red asterisk). (C) Strong expression of SASΔCyt causes mislocalization of SAS to the basal domain and cell roundness. The expanded apical membranes protrude into the lateral domain (green arrow). SAS signals are absent in the putative SJ domain (green arrowhead). (D) SAS overexpression does not affect AJs, showing intact E-Cad signals, but causes elongated SJs (cyan arrows). (E, F) SASΔCyt expression causes mislocalization of Ndg in the apical matrix (red asterisks). The basal Ndg sheet appears normal (red arrows). Scale bars: 10 ㎜.

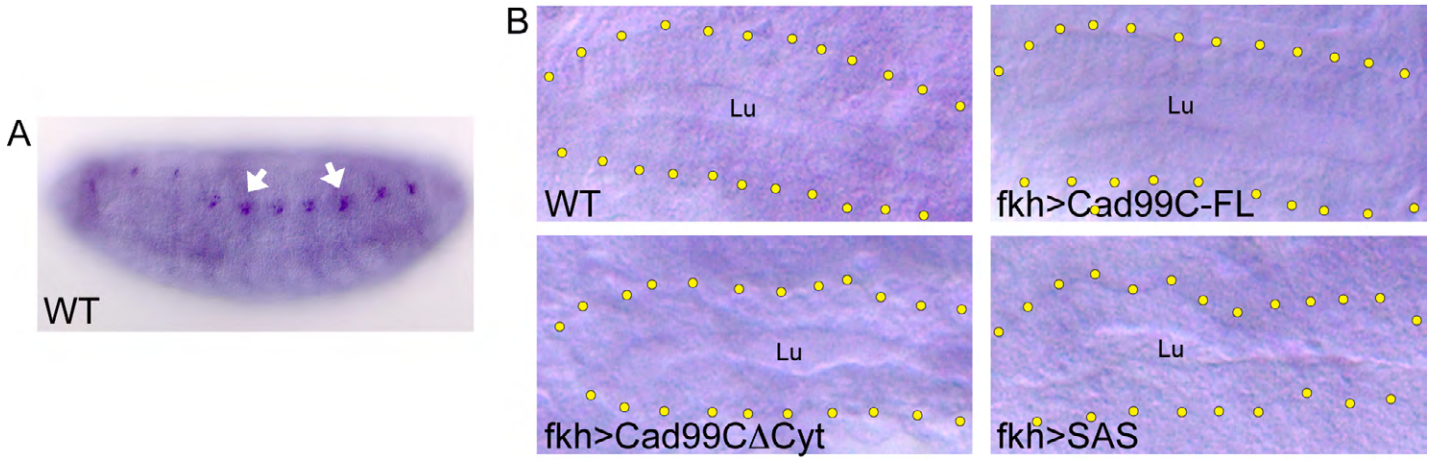


**Fig. S7. *ndg* mRNA localization is not affected by Cad99C or SAS overexpression.** (A) In situ hybridization of *ndg* against WT embryos. *ndg* is expressed in a subset of mesodermal cells (arrows). (B) Higher magnification of *ndg* in situs in the WT, Cad99C-FL-, Cad99CΔCyt- and SAS-overexpressing SGs. Yellow dots mark the gland. Lu, the lumen.